PaleoBios 28(2):41–61, September 26, 2008

Stratigraphy, paleopedology, and geochemistry of the middle Miocene Mascall Formation (type area, central Oregon, USA)

ERICK A. BESTLAND,[1] MATTHEW S. FORBES,[1] EVELYN S. KRULL,[2] GREGORY J. RETALLACK,[3] and THEODORE FREMD[4]

[1]School of Chemistry, Physics and Earth Sciences, Flinders University of South Australia, GPO Box 2100, Adelaide 5001, Australia; Erick.Bestland@Flinders.edu.au. [2]CSIRO Land and Water, Waite Laboratory, PMB 2, Glen Osmond, SA 5064, Australia; Matthew.Forbes@csiro.au, Evelyn.Krull@csiro.au. [3]Department of Geological Sciences, University of Oregon, USA; gregr@darkwing.uoregon.edu. [4]John Day Fossil Beds National Monument, National Park Service, USA; Ted_Fremd@nps.gov

The Mascall Formation in its type area has a minimum stratigraphic thickness of 353 m and consists of middle Miocene alluvial floodplain and channel deposits; its overall lithology is dominated by moderately to well-developed Alfisol-, Vertisol-, and Andisol-like paleosols that developed in a humid temperate climate. The formation is divided here into lower, middle and upper members based on conglomeratic and tuffaceous stratigraphic marker beds interpreted as cut-and-fill units that developed during episodes of climatic transition. Its depositional environment was that of a slowly aggrading alluvial floodplain consisting of fine-grained, pyroclastic-derived detritus with small fluvial channels tens of centimeters to a few meters deep. Much of the formation is organized into fining-upward sequences that are 5 to 10 meters thick each with a sandy, tuffaceous, or conglomeratic unit at its base (channel-levee deposits) and overlain by several moderately to well-developed paleosols. Based on time-of-formation estimates of the paleosols, each sequence spans a few tens of thousands of years. The sequences most likely represent climatically forced episodes of rapid floodplain aggradation (channel-levee deposits) followed by slow floodplain aggradation (paleosols). The Mascall Formation strata are geochemically similar to paleosols and volcaniclastic deposits in the Oligocene Big Basin Member of the John Day Formation. The least weathered pyroclastic strata in the formation are rhyodacitic, consisting of about 67 wt % SiO_2, 0.4 wt % TiO_2, and 7 to 8 wt. % combined bases (MgO, K_2O, Na_2O, CaO). Mass balance calculations show the well-developed paleosols have had volume collapse from the primary rhyodacitic parent of about 60%, volume collapse of about 30% when the composition of reworked tuff is used as parent, and less than 10% volume collapse from *in situ* weathering (calculated from paleosol C horizons as parent).

INTRODUCTION

The middle Miocene Mascall Formation of central Oregon is well known for its mammalian fauna, paleobotanical flora, and colorful badlands of alluvial siltstones, claystones and tuffs (Figs. 1, 2). It is now firmly established that much of the strata comprising the colorful badlands of the John Day Basin, of which the Mascall Formation is a significant part, are fossil soils (Bestland 1997, Bestland et al. 1996, 1997, Retallack et al. 2000). The Mascall Formation is thick, well-preserved, and well-exposed, contains an interesting vertebrate assemblage (Downs 1956, Fremd et al. 1997), and has a contradictory paleobotanical record (Chaney 1925, 1956). Nevertheless, minimal stratigraphic work has been done on this unit since Downs (1956) published his monograph on its paleontology and stratigraphy.

The Mascall Formation is significant because of its long and detailed paleoenvironmental record that is contained in its deposits and fossils. The fossil soils of the Mascall Formation record climatic and vegetational conditions and have not been described previously in detail (Retallack 1991a,b). Thin intrabasaltic units within the Picture Gorge subgroup, considered Mascall Formation equivalents, have been described in detail (Sheldon 2003, 2006) and the magnetic stratigraphy of the lower portion of the Mascall Formation has been established (Prothero et al. 2006). Four unpublished reports (Bestland 1994, 1998, Krull 1998, Bestland and Forbes 2003) that detail the stratigraphy of the Mascall Formation are the basis for the present contribution that integrates its fossil soil and paleontologic records. Once established, the fossil soil record and corresponding climate-vegetation-sedimentation record of the Mascall Formation can be compared to other units in and beyond the John Day Basin.

This paper presents detailed stratigraphic data on the Mascall Formation in its type area and focuses on the stratigraphic description and geochemical characterization of its numerous fossil soils. A subdivision of the formation is presented, as are distinctive types of fossil soils.

PALEOCLIMATIC SETTING OF THE MASCALL FORMATION

During the Tertiary Period, several large global climatic transitions occurred (Miller et al. 1987, Miller 1992, Zachos et al. 1991, 1993, 2001). The change from the Eocene "hot house" to the Oligocene "ice house" has been well documented (Wolfe 1978, Keigwin 1980, Prothero 1994), as has the late Miocene cooling (Hsü et al. 1977, Hodell et al. 1986). Between these two events was a remarkable middle Miocene climatic optimum that is documented from both

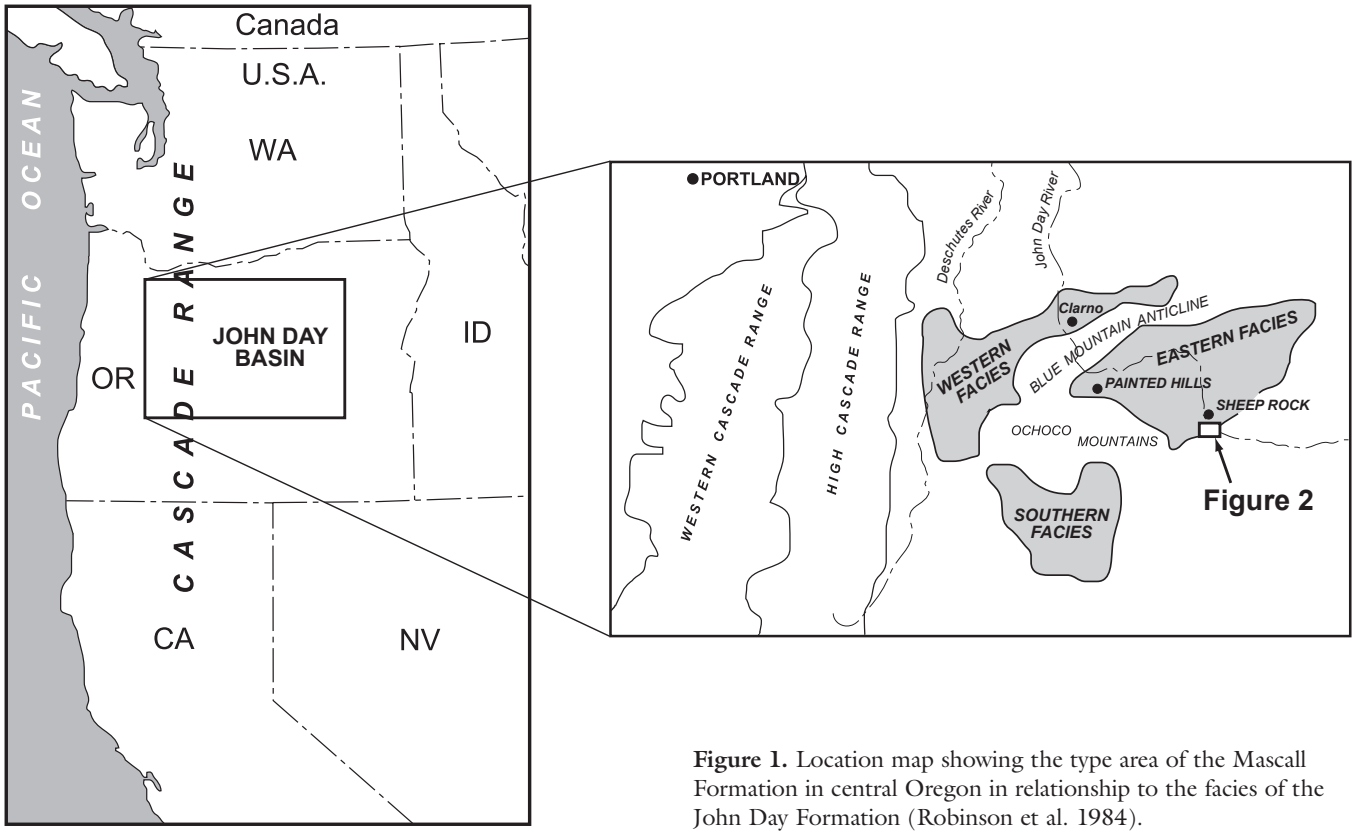

Figure 1. Location map showing the type area of the Mascall Formation in central Oregon in relationship to the facies of the John Day Formation (Robinson et al. 1984).

deep-sea cores (Woodruff et al. 1981, Woodruff and Savin 1991, Wright et al. 1992, Flower and Kennett 1994) and terrestrial sequences (Mildenhall and Pockhall 1984, 1989, Bohme 2003). The causes of this climatic optimum are controversial but could hinge on CO_2 input to the atmosphere from the eruption of the hot-spot plume head represented by the Columbia River Basalt Group (Strothers and Rampino 1990, Caldeira and Rampino 1990).

A variety of data reveals a drastic climatic change in the middle Miocene. Marine oxygen isotopes (Kennett 1986, Zachos et al. 2001) and terrestrial and marine fossils (Wolfe 1981, Itoigawa and Yamanoi 1990, Barron and Baldauf 1990, Hornibrook 1992, Bohme 2003) indicate an early middle Miocene climatic optimum (climatic optimum 1 of Tsuchi 1990, Barron and Baldauf 1990). Short duration periods of near-tropical conditions at middle latitudes around the Pacific rim are indicated by molluscs and larger foraminifera (e.g., Tsuchi 1992) and by "warm-temperate and humid" paleobotanical assemblages (e.g., Mildenhall and Pockhall 1984, 1989). This warm interval ends with climatic cooling at approximately 15 Ma; however, the cooling appears to have been stepwise, regionally variable, and may have involved carbon sequestration in organic-rich deposits such as the Monterey Formation (Vincent and Berger 1982, Flower and Kennett 1993). The onset of coastal glaciation in southern Alaska occurred at about 15–16 Ma (during climatic optimum 1) and is thought to be caused by mountain building along the coast of Alaska (Marincovich 1990). In the southern oceans, the interval just after the optimum was marked by cooling and dramatic growth of the Antarctic ice cap, as revealed by ^{18}O isotopic studies of marine foraminifera (Savin et al. 1975, Kennett 1986, Miller et al. 1987, 1991). In central Asia, the middle Miocene was a time of enhanced aridity, as revealed by eolian dust contents of deep-sea cores from the Pacific Ocean (Rea et al. 1985). In the southwestern United States, the middle Miocene was a time of decreasing humidity and the appearance of dry woodland vegetation (Axelrod 1989). A decline in mean annual temperature is evident from leaf margin studies of mixed mesophytic broadleaf floras in the Pacific Northwest (Wolfe 1981). Indications of increasingly open vegetation can be seen in the dominance of antilocaprines and horses and their increased hypsodonty in both Great Plains and western North America (Downs 1956, Webb 1977, Retallack 1997). Contrary to the Great Plains, however, paleosols of the middle Miocene Mascall Formation suggest wetter conditions than the underlying Oligocene paleosols of the John Day Formation (Bestland and Krull 1997). Thus, the marine-influenced Pacific rim location of the Miocene Mascall Formation may have had wetter conditions than the continental Great Plains.

STRATIGRAPHY OF THE MASCALL FORMATION

The Mascall Formation is here subdivided into three members (lower, middle, and upper) based on stratigraphic marker beds present in the type area (Fig. 3). The two stratigraphic breaks that subdivide the Mascall Formation probably

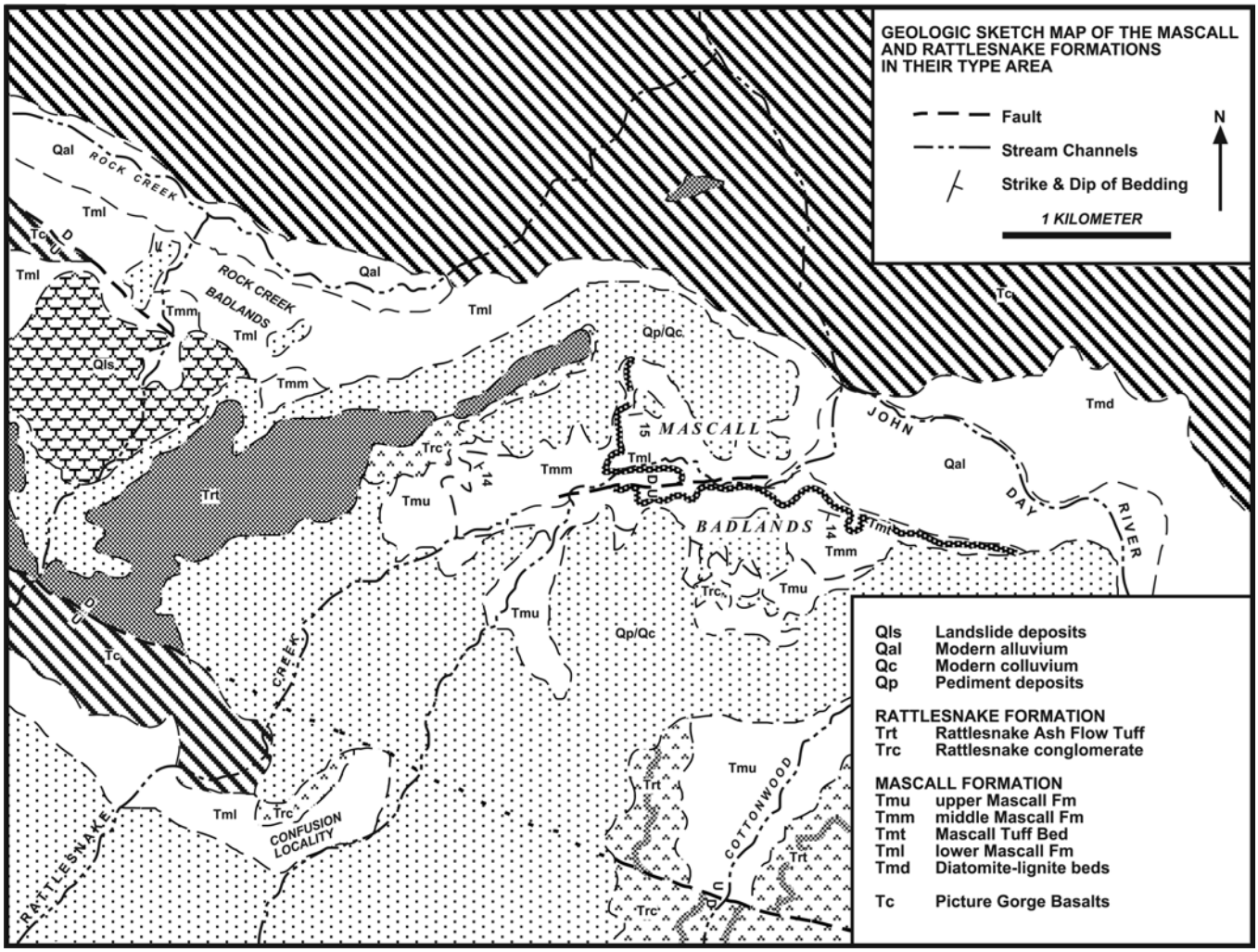

Figure 2. Geologic sketch map of the Mascall Formation in its type area.

represent climatic transitions in which there were episodes of down-cutting followed by a brief interval of rapid sedimentation before returning to slow floodplain aggradation. The formation's numerous fossil soils are grouped on the basis of distinctive megascopic features and defined as pedotypes (Retallack 1994), named using the Sahaptian Native American Language (Rigsby 1965, Delancy et al. 1988), and interpreted in terms of Soil Taxonomy (Soil Survey Staff 1975).

In its type area, the base of the Mascall Formation is conformable with the Dayville Basalt Formation of the Picture Gorge Basalt Subgroup (Bailey 1989) (Fig. 2), which have been paleomagnetically and radiometrically dated at between 16.5–16.3 Ma (million years) (Long and Duncan 1982, Hooper and Swanson 1990). A prominent tuff bed in the lower part of the Mascall Formation was dated at 16.2 ± 1.4 million years (Fiebelkorn et al. 1983). Thus, the base of the Mascall Formation is approximately 16 Ma. This lower age for the formation is in agreement with recent magnetostratigraphy by Prothero et al. (2006) that correlates normal and reversed magnetic zones in the lower Mascall Formation to Chron C5Br to C5Bn1n (16.0–14.8Ma). There is an angular unconformity of about 7–8 degrees between the Mascall Formation and the overlying upper Miocene to Pliocene Rattlesnake Formation. The Rattlesnake Formation contains the Rattlesnake Ash Flow tuff bed that forms the prominent rimrock in the John Day Valley around Dayville and has been dated at 7.05 ± 0.01 Ma (Streck and Grunder 1995, Streck et al. 1999).

There has been little revision of the stratigraphy of the Mascall Formation since it was first described by Merriam et al. (1925) and later established by Downs (1956). Merriam et al. (1925) determined a stratigraphic thickness of 2090 ft (637 m) in the type area. Downs' (1956) indication of a 390-ft (119-m) section in the type area refers only to the stratigraphic interval that he studied; he notes Thayer and Ray's (1950) report of 2000 ft (610 m). Considering the angular discordance and erosion that occurred prior to deposition of the Rattlesnake Formation and the 306 m of section that has been directly measured in the present study (Figs. 2, 3), the thickness reported by Thayer and Ray appears reasonable. The discrepancy between the directly measured section reported here and the 610 m of Thayer and Ray

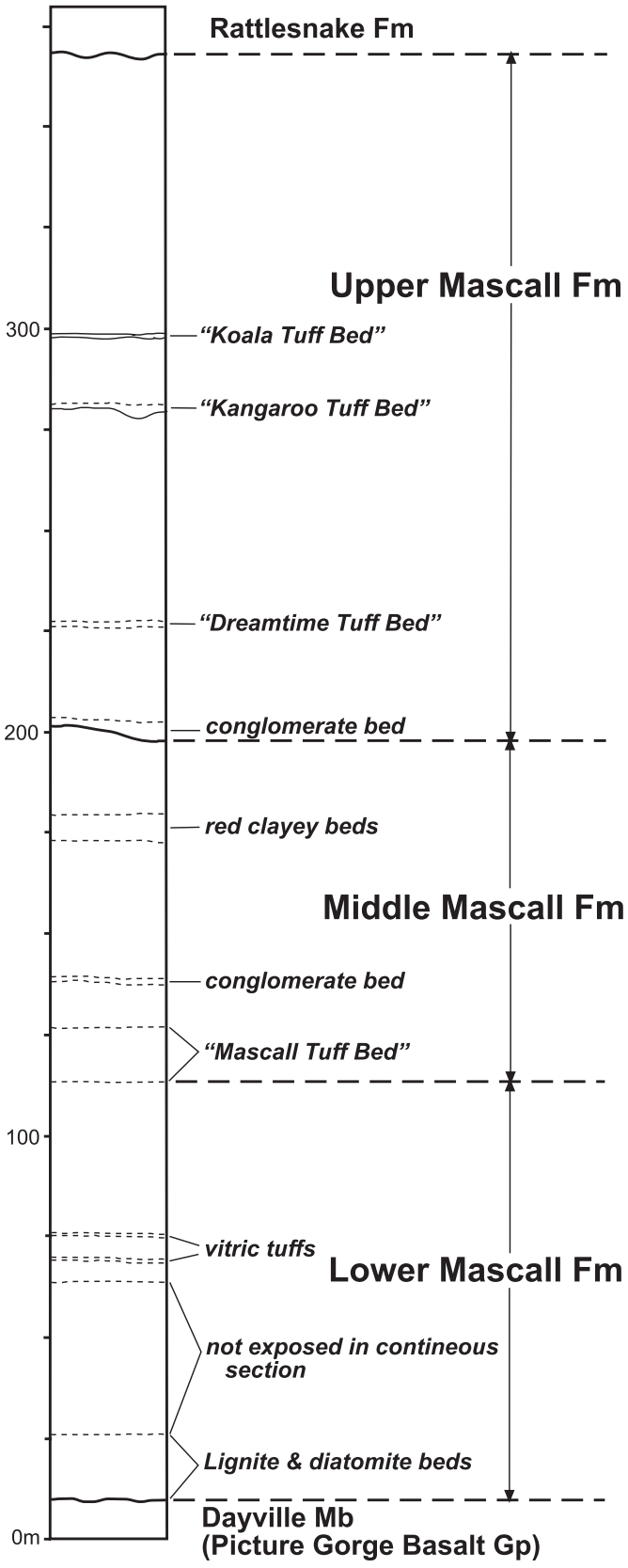

Figure 3. Stratigraphic overview of the Mascall Formation showing division between the lower, middle and upper Mascall Formation and the location of distinctive tuff and conglomerate beds.

(1950) results from the amount of covered section above the uppermost exposed Mascall Formation (Fig. 3).

Lower Mascall Formation

The lower member of the Mascall Formation consists of all beds between the upper surface of the upper flow of the Dayville Basalts and the lower surface of the Mascall Tuff Bed (Fig. 4). In the type area, this member is estimated to have a thickness of 87 m, of which approximately 46 meters is discontinuously exposed and not documented here. The Rock Creek section is composed of lithologies similar to those of the lower Mascall Formation in "The Bowl" badlands (Bestland 1998).

A lacustrine-paludal unit that is widespread along the John Day River valley and which has been a rich source of fossil leaves (Chaney 1925, 1952, 1956, Chaney and Axelrod 1959, Krull 1998), is at or close to the base of the Mascall Formation in its type area. Although extensive, these beds are not well exposed where the John Day River and Rock Creek River have formed valleys at the intersection of the resistant basalt flows and the easily eroded Mascall Formation. Several stratigraphic sections, including the 16 meters illustrated in Figure 4, were measured in a conspicuous bowl-shaped area and adjacent gullies north of the Mascall Ranch house in section 21 (Krull 1998). Here and elsewhere in the John Day-Rock Creek valleys, these beds consist of conspicuous white diatomaceous siltstones and claystones, and less abundant lignitic shales and laminated red-brown "paper shales." To the east in the John Day Valley, the stratigraphic thickness of this interval is 92 m (300 ft) (Chaney 1956, Kuiper 1988). This unit appears to be thinner in the type area, where complete exposures of this interval are lacking.

Previous studies of diatoms in the Mascall Formation report a flora dominated by *Aulacosira ambigua*, *Aulacosira granulata*, and *Melosira teres*, with *Aulacosira ambigua* the most abundant (Kuiper 1988). Abundant *Melosira*, particularly *M. granulata* and *M. paucipunctata*, occur elsewhere in central Oregon (Oliver 1936). *Melosira* is characteristic of freshwater lakes that have low amounts of dissolved solids (salts) and it is commonly the first genus that invades lakes (Oliver 1936, van Landingham 1964). The occurrence of this cosmopolitan planktic diatom is evidence for slightly alkaline freshwater and eutrophic conditions (Taylor et al. 1990).

Above the diatomaceous-lignitic interval are silty claystone and clayey tuffaceous horizons, both with abundant pedogenic clay structures, and several conspicuous, thin, gray tuff beds (Fig. 4). A distinctive sequence of deposits common throughout the Mascall Formation consists of maturing-upward fossil soils with tuffaceous strata at the base and clayey strata toward the top. Several of these sequences are present in the lower Mascall Formation section. From 66 m to 71 m, there is a classic maturing-upward fossil soil sequence that consists of Inceptisol-like, then Alfisol-like and Vertisol-like paleosols capped by a tuffaceous sandstone bed. This sandstone is overlain by a well-sorted, coarse siltstone with large

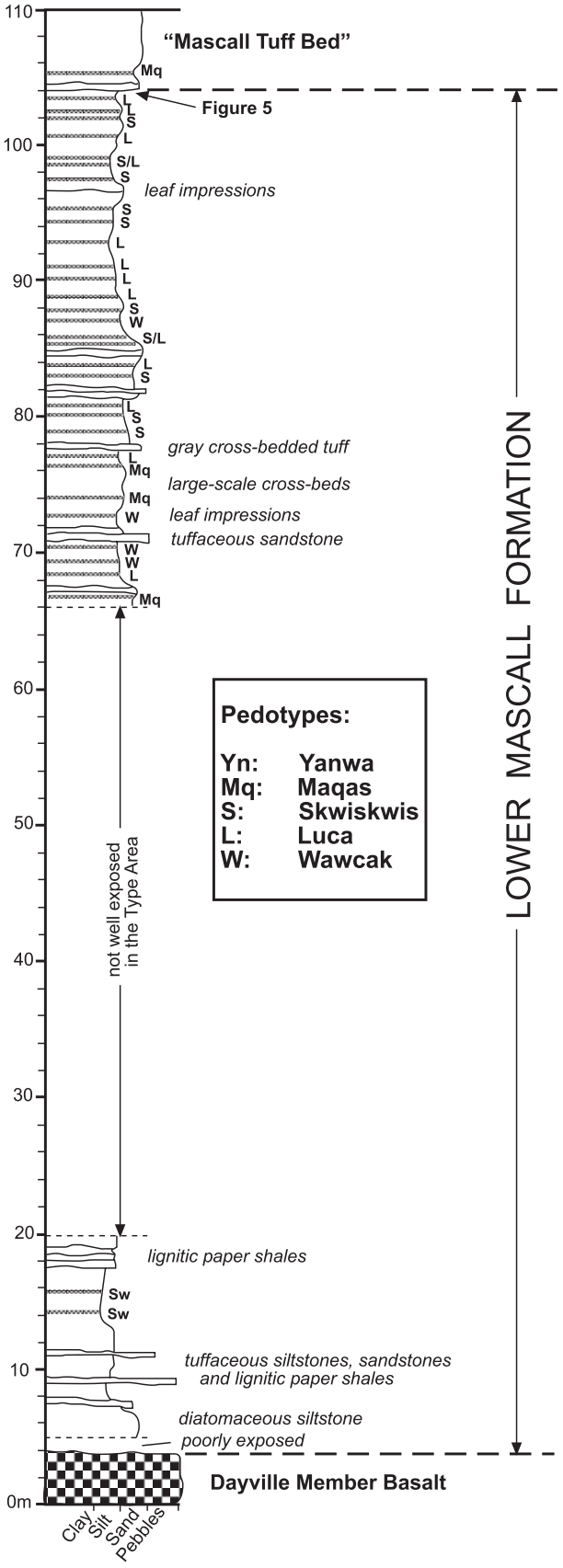

Figure 4. Stratigraphy of the lower Mascall Formation. Pedotype abbreviations are used in Figures 6 and 9.

(meter-scale) cross-bedding, which has been interpreted as an eolian dune. This "dune" is overlain at the 76–77 m level by another maturing-upward fossil soil sequence capped at 78 m by a cross-bedded, tuffaceous silt. A third fossil soil sequence is capped by Alfisol-like paleosol at the 82 m level (Fig. 4). This paleosol is overlain by a bedded gray tuffaceous siltstone interval that begins the next sequence. A lithologic break occurs at 104 m between well-developed and structured clayey fossil soils that contain minor amounts of tuffaceous horizons and the massive Mascall Tuff Bed (Fig. 5B, C). This horizon defines the boundary between the lower and middle Mascall Formation.

Middle Mascall Formation

The middle Mascall Formation consists of all beds from the base of the Mascall Tuff Bed to the contact with the conglomeratic bed that caps the member. In the Mascall badlands, this member is approximately 87 m thick and continuously exposed (Fig. 6). The Mascall Tuff Bed is a massive, fine-grained, very crystal-poor, tuffaceous siltstone. It contains some stratified tuffs with interbedded Inceptisol-like fossil soil at its base. The tuff bed has an upper section with Inceptisol-like fossil soils that are vaguely horizonated, burrowed, and full of root traces (Fig. 7A, B). Conglomeratic lenses with pumiceous and pedogenic clasts are common in the upper part of the Mascall Tuff Bed. These fossil soils and conglomerates were examined in detail (Bestland 1998) because they are the lowest major conglomeratic horizon in the Mascall Formation. The fossil soils have a texture (observed in thin-section) that consists of bridged and thinly coated soil voids. The texture is distinctive because it consists of numerous, fine- to medium-sized voids (0.05 to 0.5 mm) that have discrete clay walls.

Above the Mascall Tuff Bed, the dominant lithologies of silty claystones and tuffaceous claystones (Fig. 7C, Fig. 8A, B) are interbedded with distinct pedolithic conglomerates or sandstones. The middle Mascall Formation has the most conglomeratic beds of the three Mascall members. Whereas the lower and upper members have depositional sequences punctuated by tuffaceous or tuff beds, the middle member has many sequences punctuated by conglomeratic beds. The clasts in these conglomerates and coarse sandstones are apparently tuffaceous, as they are well-rounded, friable, and light-colored. The clasts weather out of the rock intact but, unlike basaltic and welded tuff clasts, they do not endure downstream transport in gullies for more than a few tens of meters. When broken, most of these clasts reveal ancient root traces. In thin-section, most of the clasts do not have a pumiceous texture, but instead are stained with iron oxides (Fig. 8C, D). Many clasts show internal conglomeratic textures of clasts within clasts. Neither dilute HCl nor thin-sectioning (62 thin sections cut from Mascall Formation) revealed the presence of calcium carbonate cement. Thus, the root traces, clast within clast morphology, and iron-oxide cement indicate that these clasts are from subsurface soil horizons that

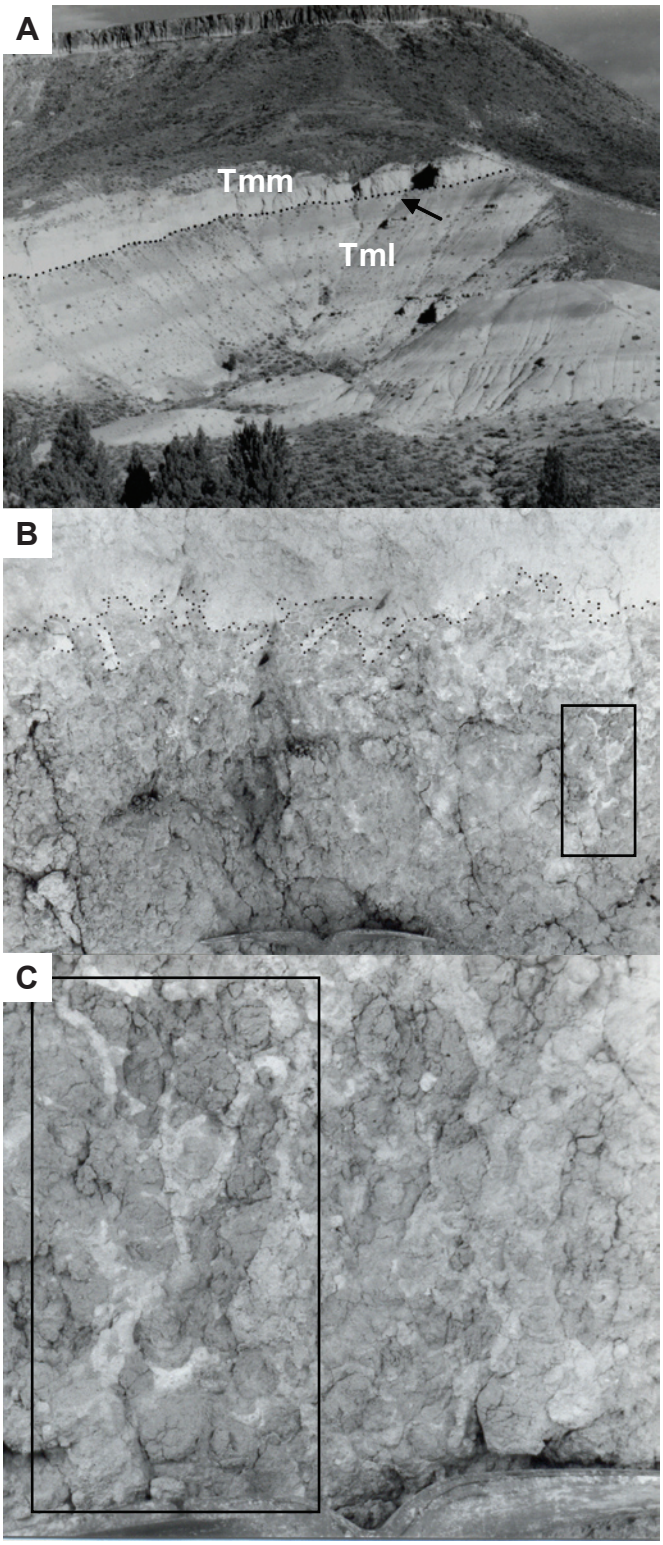

Figure 5. Photographs of the lower Mascall Formation from "The Bowl" area of the Mascall badlands. **A**, The Mascall Tuff Bed defines the boundary between the lower and middle Mascall Formation. Rattlesnake Tuff Bed caps hill. **B**, Interdigitating contact between fossil soil Bw horizon (lower), with numerous burrow structures, and the massive tuff (upper) of the Mascall Tuff Bed. **C**, Close-up of burrowed features (digging tool is 33 cm across).

became weakly cemented. They were then eroded, rounded, and rapidly deposited as channel lags.

The middle Mascall Formation is also notable for the deep red-brown hues of its fossil soil horizons (7.5–5YR; Munsell Color 1975). In contrast, fossil soils in the lower and upper Mascall Formation are 10YR–2.5Y brown. The most prominent red-brown fossil soil is a 10-m thick interval of well-structured clay (Fig. 6). The pedogenic clay structures and color of these fossil soils indicate well-drained conditions for this part of the Mascall Formation floodplain. Fossil soil features are discussed below.

Upper Mascall Formation

The upper Mascall Formation is defined as all beds from the base of a prominent conglomerate interval or its lateral equivalent to truncation of the unit by its angular unconformity with the Rattlesnake Formation (Fig. 9, Fig. 10A, B). In the Mascall badlands, the upper Mascall Formation is the best exposed of the three members and it consists of a minimum of 165 m of strata. The upper member is thicker than the 165 m measured here due to the angular unconformity between the Mascall and Rattlesnake formations and lack of exposure of this part of the section.

The upper member has the same lithologies as the lower members, including silty claystone, tuffaceous claystone, pedolithic conglomerates, and tuff. It contains abundant Vertisol-like fossil soils that are distinguished by their very clayey character, large subhorizontal clay structures, and olive color. Several tuff beds are exposed in the badlands and are informally named here as "Dreamtime Tuff," "Kangaroo Tuff," and "Koala Tuff." These are potential marker beds that may help correlate the type section with other Mascall-like sections. The "Dreamtime Tuff" is a very light grey, fine-grained, crystal-poor, vitric tuff that is about one meter thick with indistinct bedding toward the base and grading upward and into the overlying fossil soil. The "Kangaroo Tuff" is a very pale yellow, fine-grained, crystal-poor, vitric tuff that ranges from 20 cm to several meters, and is thickest where it fills channels. The "Koala Tuff" is a very pale yellow, fine-grained, crystal-poor, vitric tuff that is about one meter thick and with some thin bedding.

DESCRIPTION AND GEOCHEMISTRY OF THE PALEOSOLS

Utilizing the pedotype concept (Retallack 1994) and previous work on John Day Basin paleosols (Bestland et al. 1996, 1997, Bestland 1997, Retallack et al. 2000), six major pedotypes or types of paleosols are recognized in the Mascall Formation (Table 1, Fig. 11). All but the Walasx have been previously defined from the John Day Formation. The vast majority of Mascall Formation paleosols examined in the type area belong to the Maqas, Patu, Skwiskwi, Luca, and Wawcak pedotypes. These pedotypes are interpreted as a developmental sequence of paleosols, from weakly developed tuffaceous Entisol- and Inceptisol-like paleosols to pedogenically well-

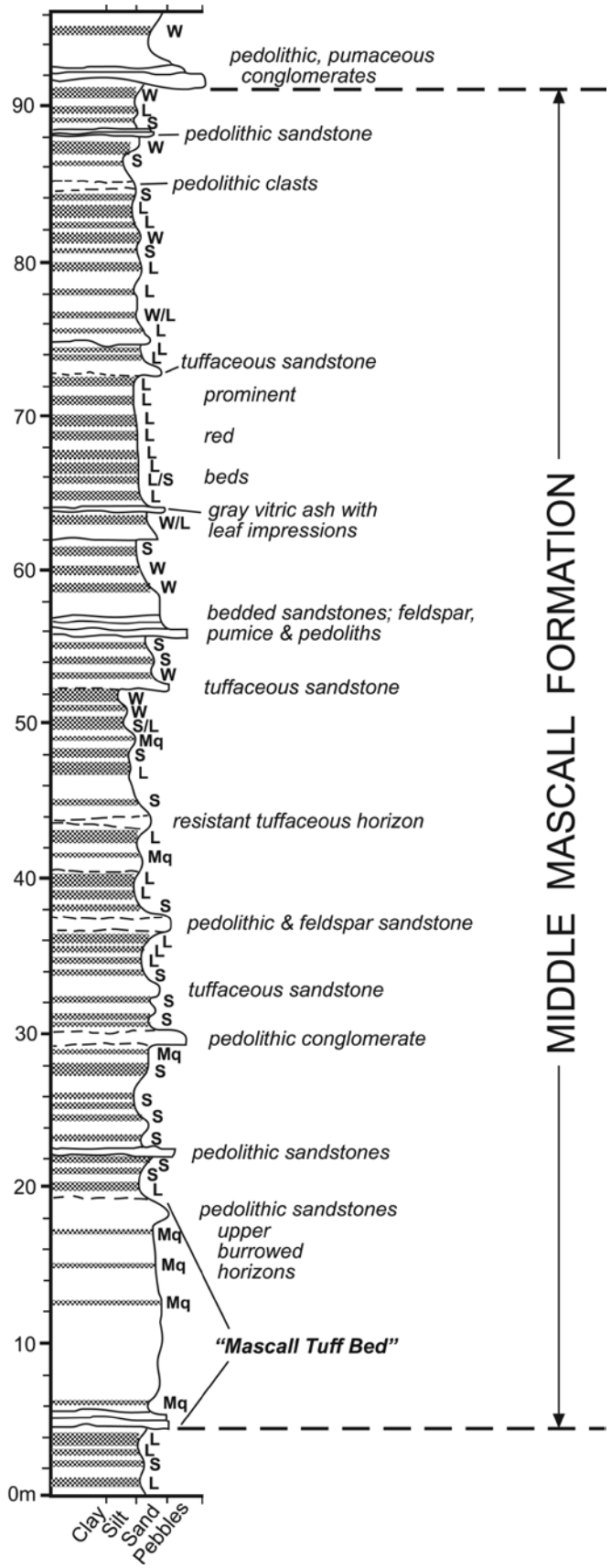

Figure 6. Stratigraphy of the middle Mascall Formation. See Figure 4 for pedotype abbreviations.

structured, clayey Vertisol- and Alfisol-like paleosols. The least developed and least horizonated of these paleosols are the Kwalk and Skaw pedotypes, interpreted as sandy-tuffaceous and silty-clayey Entisol-like paleosols, respectively. These are followed by the Maqas pedotype, an andic Inceptisol-like

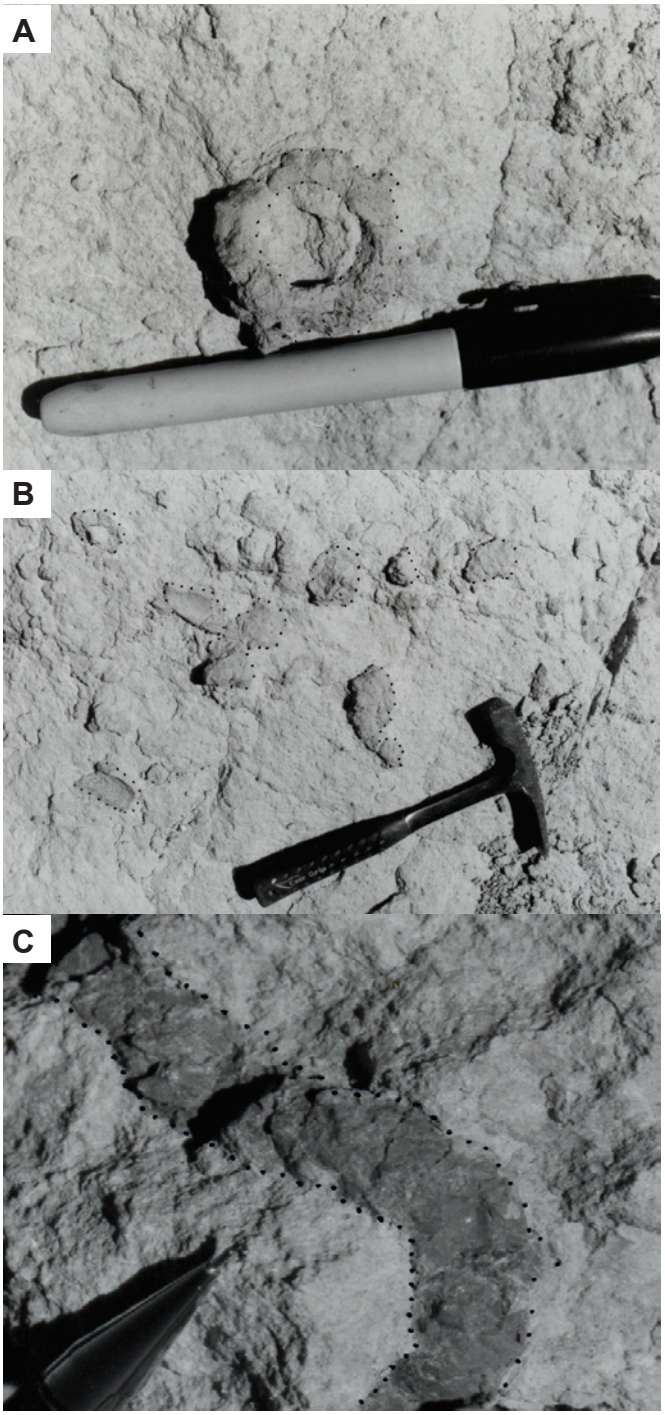

Figure 7. A and **B.** Photographs of burrow structures in the upper part of the Mascall Tuff Bed, middle Mascall Formation. **C.** Clay-filled burrow structure in a C horizon from the sequence of Luca fossil soils in the middle Mascall Formation.

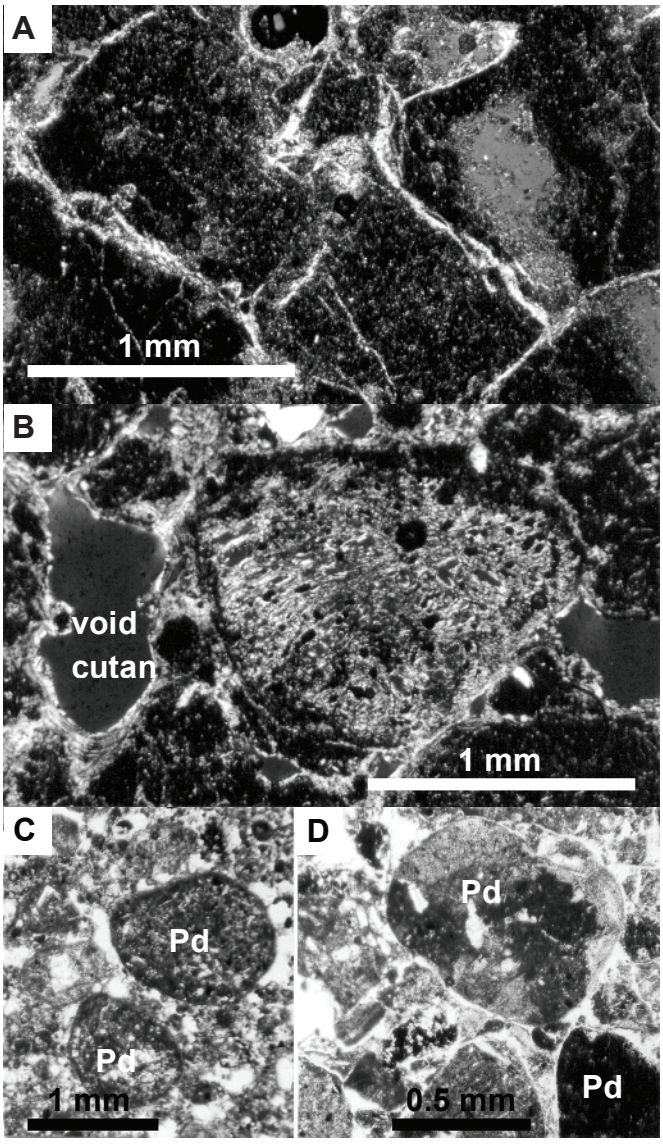

Figure 8. Photomicrographs of Mascall Formation units. **A.** Well-developed argillans (clayskins) define subangular blocky structure in a Luca paleosol. **B.** Void cutan with preserved void space and pumice fragment from a Skwiskwis paleosol. **C.** Rounded pedolithic clasts (Pd) in conglomeratic beds in the middle Mascall Formation. **D.** Iron-stained and clayey pedolithic clasts (Pd) with thin argillan coatings from a Maqas paleosol.

paleosol and the Patu pedotype, a mollic Inceptisol-like paleosol. Intermediate between the Inceptisol-like Maqas and Patu and the Alfisol- and Vertisol-like paleosols is the clayey, vitric, Andisol-like paleosol of the Walasx pedotype. Increasing in clay content, the next paleosol in the sequence is the andic Alfisol-like Skwiskwi pedotype. Depending on the type of pedogenic clay structure and color, the Luca and Wawcak pedotypes follow in the sequence. The Luca pedotype (Alfisol-like paleosol) is red-brown and clayey with blocky clay structures, whereas the Wawcak pedotype (Vertisol-like paleosol) is olive brown and clayey with coarse sub-horizontal clay structures.

Thin-section examination revealed pedogenic features such as the presence of original ped, cutan, and void cutan structures (Fig. 8A, B). It also revealed the pedogenic origin of distinctive conglomeratic clasts common in the Mascall Formation, and a lack of diagenetic features such as the recrystallization of vitric material or of clays. It can therefore be concluded from the petrographic study that the only diagenetic changes have been compaction and organic matter decomposition. No features attributable to groundwater, such as cements, were observed. This relatively pristine state supports the geochemical analysis presented below and which endeavors to interpret the geochemical data in terms of original pedogenic processes.

Maqas and Patu Pedotypse

Ubiquitous in the Mascall Formation are very pale brown (10YR), silty, tuffaceous horizons interpreted as andic Inceptisol-like paleosols. Maqas paleosols were originally defined from the Turtle Cove Member of the John Day Formation with the type profile below Carrol Rim in the Painted Hills (Retallack et al. 2000). Maqas paleosols are better preserved in the Mascall Formation than in the John Day Formation due to their lesser depth and time of burial. Unlike most of the John Day Formation, Mascall Formation strata have not been zeolitized (Hay 1963). With an increase in granular and crumb ped structure, Maqas paleosols grade into Patu paleosols. Patu paleosols are interpreted as mollic, andic Inceptisol-like paleosls (Retallack 2004).

Maqas and Patu paleosols in the Mascall Formation are weakly horizonated with a subsurface horizon of slight clay accumulation and root traces interpreted as a Bw (cambic horizon). Root traces are commonly coated with clayey material and tuffaceous components are commonly bridged with clayey material. The tuffaceous character as well as the low clay content causes these horizons to be more resistant to erosion than horizons with higher clay contents. Maqas paleosols can contain friable, rounded clasts of pedolithic origin. These paleosols are geochemically similar to a rhyodacitic composition with the notable exceptions of having higher TiO_2 and Fe_2O_3 contents and lower SiO_2 content (Figs. 11, 12).

Walasx Pedotype

A distinctive type of pale yellow (5Y) tuffaceous claystone with medium columnar ped structure, a secondary set of angular blocky peds, and translucent clay films is here named the Walasx pedotype. This type of paleosol has not been previously defined and is named after the Sahaptin word Walasx, meaning pine gum or resin, in reference to the translucent clay films. It is interpreted as an Andisol based on its tuffaceous component and its translucent clay films that are interpreted as forming from amorphous weathering products such as allophone. The type pedotype has a narrow (30 cm thick) clay-rich B horizon between a tuffaceous sandstone above and a tuffaceous siltstone of the C horizon below. Walasx paleosols are moderately

Table 1. Pedotypes, their descriptions, geochemical summary, and interpretations of soil analogues for the Mascall Formation.

Name/Meaning	Description/Interpretation	Al/Bases	Fe_2O_3 wt. %	TiO_2 wt. %
Maqas/Patu (Yellow/Fine)	Pale yellow (5Y7/4) to pale brown (10YR) tuffaceous clayey siltstone with abundant hollow root traces and other soil voids; surface horizons A, Bw (10–30 cm) with clay coated peds and root trace surfaces over resistant subsurface tuffaceous siltsone (C or Csi horizons). **Soil Development:** weak-moderate **Soil Identification:** vitric Inceptisol/ mollic Inceptisol	0.8–2.2	5.0–5.9	0.8–0.9
Walasx (Resin)	Pale yellow (5Y7/3) tuffaceous claystone with translucent clay films on voids and root traces; surface horizons A and Bt or Bw of 30 cm overly tuffaceous siltstone C horizon. **Soil Development:** moderate **Soil Identification:** Andisol	2.2–2.6	7.2	1.2
Skwiskwi (Brown)	Red-brown (10YR4/3) silty claystones with A-Bt-C profile; thick surface zone (30cm) with common tuffaceous component and crumb peds over subsurface horizon (Bt) enriched in clay with a variety of clay structures (subangular blocky, columnar) over pale olive (5Y6/3) clayey siltstone (C horizon). **Soil Development:** moderate **Soil Identification:** vitric Alfisol	1.2–1.8	6.1–9.9	1.1–1.3
Luca (Red)	Red-brown (7.5–5YR) silty claystones with well-structured Bt horizon consisting of subangular blocky peds and cutans; minor tuffaceous component; commonly cumulative. **Soil Development:** moderate-strong **Soil Identification:** Alfisol	2.6	6.1–9.9	1.1–1.3
Wawcak (Split)	Pale yellow (5Y7/4) to pale olive (5Y6/3) clayey A-C horizons or Bt horizon with convoluted, subhorizontal, coarse clayskins and cutans up to 60 cm thick. **Soil Development:** moderate-strong **Soil Identification:** Vertisol	2.8–3.4	6.0–9.1	1.2–1.3

horizonated, having well-developed clay structures, but still retain a strong tuffaceous component. This paleosol has similar characteristics to andic Alfisol-like paleosols of the Skwiskwi pedotype described below (Figs. 11, 12).

Skwiskwi Pedotype

Ubiquitous in the Mascall Formation are brown (10YR) silty claystone horizons of the Skwiskwi pedotype, interpreted as andic Alfisol-like paleosols. The type Skwiskwi paleosol is in the Oligocene Big Basin Member of the John Day Formation in the Painted Hills area (Retallack et al. 2000). B horizons of Skwiskwi paleosols in the Mascall Formation are very well structured with medium angular blocky ped structure and medium-fine blocky to crumb structure. Some Skwiskwi paleosols have columnar ped structure as well, similar to the Walasx paleosols that they grade into. With increasing clay content, red color, and dominance of subangular blocky ped structure, Skwiskwi paleosols grade into Luca paleosols (described below). Skwiskwi paleosols are geochemically similar to Walasx and Luca paleosols.

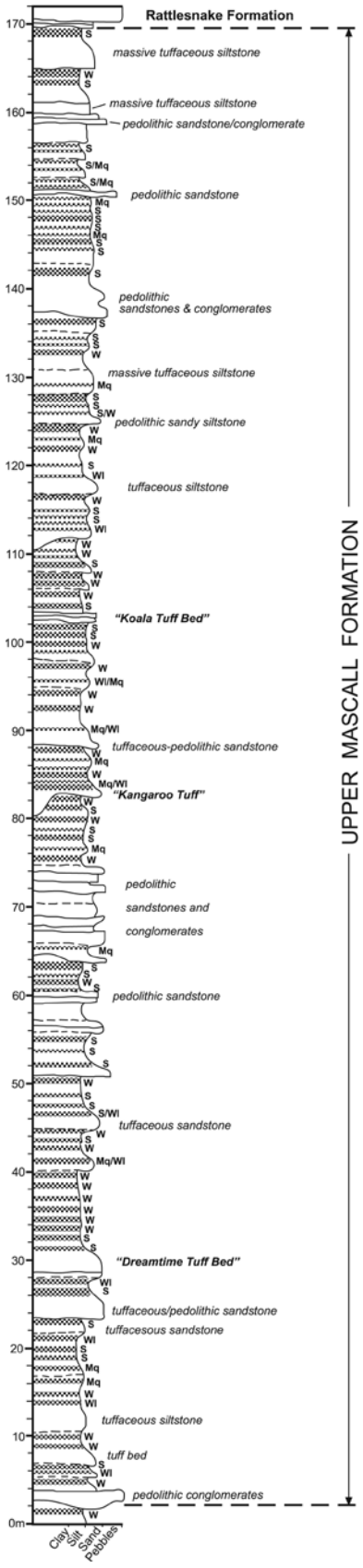

Figure 9. Stratigraphy of the upper Mascall Formation. See Figure 4 for pedotype abbreviations.

Luca Pedotype

Common in the middle Mascall Formation and less common in the upper and lower members are red-brown, silty claystone horizons of the Luca pedotype, interpreted as Alfisol-like paleosols. The type Luca paleosol occurs in the late Eocene part of the John Day Formation in the Camp Hancock area (Retallack et al. 2000). B horizons of this paleosol type in the Mascall Formation contain well-developed subangular blocky ped structure with subordinate finer ped structures. A prominent set of about 10 meters of red-brown claystones outcrops in low mounds in the center of the Mascall Badlands and consists of cumulic B horizons of Luca paleosols. These paleosols are geochemically more weathered than Walasx and Skwiskwi paleosols (Table 1).

Wawcak Pedotype

Dominating the strata of the upper Mascall Formation and common in the other two members are brown and olive brown (2.5Y–5Y) silty claystones and claystone horizons of the Wawcak pedotype, interpreted as Vertisol-like paleosols. The type Wawcak paleosol is in the lower Oligocene part of the John Day Formation in the Painted Hills area (Retallack et al. 2000). The distinctive feature of this pedotype in the Mascall Formation is the large (coarse to very coarse, up to 10 cm), and abundant subhorizontal clay skins. The clay skins are commonly slickensided and define coarse lentil-shaped peds, characteristic of Vertisols. They are the most clay-rich paleosols in the Mascall Formation, forming benches in the eroding badlands. Geochemically, these are the most weathered paleosols (Fig. 11, Table 1).

Yanwa/Monana Pedotypes

Restricted to the thin interval of diatomaceous and lignitic beds at the base of the Mascall Formation are brown lignitic beds over very pale yellow clay of the Yanwa pedotype, interpreted as histic Inceptisols. A very similar type of paleosol occurs in the lower Oligocene part of John Day Formation in the Painted Hills area which is the type pedotype (Retallack et al. 2000). As in the Oligocene part of the John Day Formation, these paleosols are interpreted as forested swamp soils, marginal to lakes or ponds. The Monana pedotype (Retallack 2004) occurs elsewhere in the upper part of the Mascall Formation (Retallack 2004) and is darker colored than the Yanwa pedotype. Monana paleosols probably resulted from coniferous and dicot leaf debris whereas the Yanwa were dominated by coniferous (*Metasequoia occidentalis*) leaf debris (Retallack et al. 2000).

Geochemistry

Geochemical analysis (x-ray fluorescence of bulk rock samples) of 62 samples from throughout the Mascall Formation has enabled evaluation of the degree and direction of weathering recorded in these paleosols (Tables 2, 3). Direction of weathering refers to soil-forming processes that cause either loss or accumulation of elements during weathering.

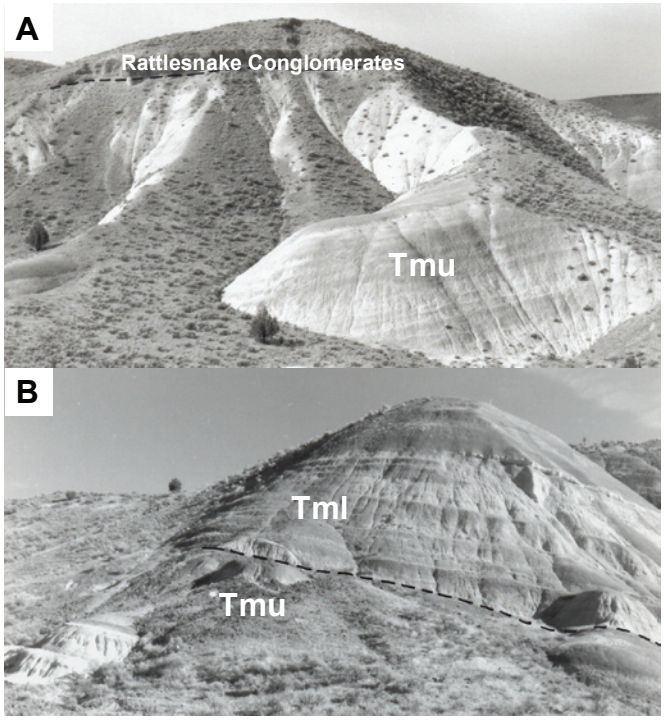

Figure 10. Lithostratigraphic boundaries within the Mascall Formation. **A.** Photograph of the angular discordance between the upper Mascall Formation and the overlying Rattlesnake Formation in the Mascall Badlands. **B.** Boundary between the upper and middle Mascall Formation is defined at the base of a laterally continuous channel conglomerate unit (resistant unit above dashed line).

Examples of common geochemical weathering changes would be base cation loss in humid climate soils or iron and titanium accumulation in soils that are not waterlogged. In this paper, the term weathering is also used to refer to geochemical changes that have occurred to alluvial and colluvial detritus en route to the depositional basin and prior to final deposition. This model of weathering is similar to those used to evaluate whole catchment weathering and has been used before in the weathering analysis of John Day Basin strata (Bestland 2000). This type of weathering model is appropriate for John Day Basin strata because the dominant detritus type is airfall pyroclastic detritus, and as such, its composition can be determined and averaged (Bestland 2000). It has been shown that in many aggrading alluvial environments, such as the Mascall basin, most weathering, in terms of elemental loss and gain, occurs prior to final deposition. Weathering of this sort is especially true of volcanic (pyroclastic) detritus that has high initial weathering rates due to the instability of volcanic materials in most weathering environments. High weathering rates are due to the non-crystalline nature of most pyroclastic materials as well as the high surface area of the detritus.

Geochemical scatter plots of major elements involved in common soil weathering scenarios are presented in Figure 12. The samples are separated into three categories based on their geochemistry: (1) B-horizons of Vertisol and Afisol-like paleosols, (2) tuffaceous Inceptisol-like paleosols, tuffaceous C-horizons, and tuffaceous alluvial deposits, and (3) a tuffaceous horizon with a geochemistry closest to unweathered volcanic material of rhyodacitic composition and referred to as "primary parent." Clear weathering trends are present and illustrate desilication, base cation loss (Fig. 12A), immobile element accumulation (TiO_2) corresponding to desilication (Fig. 12B), and alumina concentration corresponding to immobile element accumulation (Fig. 12C). Significant elemental differences are present between the parent tuff composition, tuffaceous units, and clayey paleosol B-horizons and are interpreted as representing hydrolysis weathering releasing silica and base cations to soil solution at the same time relatively stable clay minerals are formed. The formation of clay slows the removal of alumina, and to an extent silica, from the soil. Tuffaceous horizons and deposits show a marked loss of silica with a minimal loss of base cations (Fig. 12A). Conversely, the clayey paleosol B-horizons show marked loss of base cations with little change in silica. Apparently, desilication is the dominant weathering process in tuffaceous materials, whereas most base cation loss occurs after clay minerals form. This interpretation is reinforced by the steady increase in alumina concentration compared to titania content (Fig. 12C). The correspondence between alumina and titania contents most likely indicates clay mineral formation along with immobile element concentration. In contrast, there is poor correspondence between titania and silica in paleosol B horizons (Fig. 12B), probably indicating that mixtures of tuffaceous components in the horizons are obscuring the expected weathering trend of increased titania corresponding to decrease of silica as clay minerals form at the expense of volcanic glass.

Mass Balance Analysis of Weathering—Quantification of the degree and direction of weathering can be made by considering pedogenic strain and mass transfer, following mass balance techniques for soil and paleosols (Brimhall and Dietrich 1987, Brimhall et al. 1991, Chadwick et al. 1990, Bestland et al. 1996). Pedogenic strain is the overall volume change due to weathering calculated based on the assumption of elemental immobility (commonly Ti and or Zr) and the assumption of a parent material composition. Pedogenic strain is defined as $[\rho_{i,w}=(\rho_p C_{i,p}/\rho_w C_{i,w})-1]$ where i indicates immobile element, C is concentration in weight percent, ρ is density, w is weathered daughter, and p is parent. "Normal" weathering processes of hydrolysis and leaching generally cause volume loss, termed collapse (Fig. 13). Soils which have material added during weathering from floods and or wetfall-dryfall sources can show volume gain, termed dilation, if this amount is greater than weathering losses. Mass transfer of individual elements is similarly based on immobile element assumptions and assesses the gain or loss of elements compared to a parent. Pedogenic mass transport is defined as $[\rho_{j,w}=(\rho_p C_{i,p}/\rho_w C_{i,w})(\rho_{i,w}+1)-1]$, where j is the element in question. Elements can be lost or concentrated

Table 2. XRF data and bulk densities determined for selected tuffaceous beds and paleosol horizons from throughout the Mascall Formation. All values are weight percents except for Zr which is ppm.

Sample	Hzn	SiO_2	Al_2O_3	Fe_2O_3	MgO	CaO	Na_2O	K_2O	TiO_2	P_2O_5	Zr	LOI	Total	Bulk d
1d1	C	55.70	16.20	6.86	1.46	3.58	1.43	0.84	1.07	0.77	212.7	9.27	98.69	1.36
1d2	C	57.49	16.52	7.02	1.42	3.79	1.37	0.91	1.08	0.88	224.6	9.06	99.69	1.48
1d3	B	58.83	16.86	6.88	1.39	2.99	1.32	0.92	1.08	0.41	238.3	8.75	99.63	1.53
1d4	Bt	58.28	16.54	9.21	1.54	1.88	0.83	0.74	1.27	0.04	252.8	9.58	100.0	1.86
1d5	Bt	58.71	16.73	9.05	1.55	1.91	0.87	0.76	1.27	0.04	253.4	9.09	100.1	1.81
1d6	Bt	58.39	16.58	8.90	1.54	1.91	0.86	0.74	1.27	0.04	249.8	9.47	99.81	2.00
1d7	C	58.20	16.68	8.93	1.52	2.03	0.94	0.76	1.25	0.05	246.0	9.19	99.69	1.79
1d8	C	59.95	17.40	6.57	1.08	3.15	2.38	1.12	1.28	0.06	250.8	6.54	99.64	1.73
2d1	C	58.33	17.16	8.07	1.32	2.02	1.31	0.91	1.27	0.04	264.8	8.78	99.30	1.82
2d2	Bt	57.93	17.25	8.41	1.34	2.01	1.04	0.78	1.30	0.09	267.3	9.53	99.79	1.80
2d3	Bt	57.56	17.19	8.47	1.35	2.06	0.95	0.76	1.27	0.19	254.6	9.72	99.75	1.88
2d4	Bt	58.63	17.07	8.22	1.34	1.95	0.96	0.74	1.28	0.12	258.7	9.26	99.66	1.85
2d5	Bt	57.12	17.92	8.37	1.27	1.72	0.86	0.63	1.29	0.05	269.6	9.60	98.87	1.83
2d6	B	57.62	17.61	8.86	1.30	1.74	0.85	0.63	1.28	0.06	261.1	9.47	99.53	1.77
2d7	C	59.48	17.50	7.48	0.92	2.36	1.81	0.79	1.24	0.06	274.5	8.11	99.85	1.68
3d1	C	59.73	16.77	7.08	1.07	2.55	1.92	1.03	1.15	0.06	255.8	8.29	99.75	1.59
3d2	C	59.11	16.27	7.21	1.05	2.48	1.68	0.97	1.17	0.06	257.6	8.66	99.32	1.57
3d3	Bt	59.68	16.92	7.04	1.05	2.56	1.87	0.99	1.18	0.05	264.6	8.10	99.53	1.66
3d4	Bt	59.05	17.50	7.25	1.14	2.91	1.85	0.78	1.24	0.07	219.8	7.73	99.61	1.46
3d5	Bt	58.74	17.68	7.13	1.12	2.84	1.77	0.70	1.20	0.07	221.8	8.60	99.94	1.53
3d6	C	66.81	14.01	2.85	0.49	1.87	2.35	2.83	0.52	0.07	306.2	7.00	98.97	1.34
4d1	C	57.89	17.97	6.26	1.36	3.25	1.86	1.07	1.23	0.05	250.1	8.26	99.37	1.68
4d2	C	57.30	16.97	8.90	1.73	2.45	1.05	0.94	1.24	0.04	246.6	9.02	99.71	1.94
4d3	Bt	57.01	16.96	8.69	1.71	2.61	0.97	0.99	1.22	0.04	252.7	9.37	99.71	1.88
4d4	Bt	57.09	16.80	8.50	1.74	2.71	1.02	1.04	1.19	0.03	253.0	9.49	99.71	1.95
4d5	Bt	57.63	16.87	8.29	1.66	2.83	1.24	1.12	1.17	0.04	250.1	9.01	100.0	1.80
4d6	Bt	57.15	16.56	8.54	1.71	2.77	1.17	1.08	1.18	0.04	251.2	9.28	99.60	1.92
5d1	C	62.21	16.30	5.84	1.11	3.03	1.94	1.35	0.89	0.08	235.9	6.82	99.66	1.46
5d2	B	61.06	16.53	5.92	1.18	3.01	2.05	1.33	0.87	0.26	228.6	6.92	99.31	1.52
5d3	C	63.13	15.89	5.59	1.06	2.97	1.95	1.44	0.86	0.08	233.9	6.68	99.73	1.40

(addition) due to weathering processes. For example, base cations, silica, and even alumina are generally lost during hydrolysis weathering (Fig. 13A, B), whereas iron is generally concentrated (addition) (Fig. 14A). The concentration of iron demonstrates the immobility of iron in most oxidizing soil environments. Conversely, alumina is lost due to hydrolysis weathering but not nearly to the same extent as silica. These trends are discussed below.

Parent material compositions are of utmost importance in these calculations and are not commonly easily identified. One candidate for parent material is to choose the C horizon of the fossil soil, and is termed *in situ* parent (Fig. 13A). This choice ignores the cumulative nature of soil development common to aggrading alluvial systems; the C horizon chosen for a parent was most likely a B horizon prior to soil aggradation, thus allowing for the possibility that the parent could have a higher degree of weathering than the B horizon in question. Another candidate for parent material is to choose alluvial deposits that show the least amount of pedogenic modification. Candidates for this type of parent would be deposits that show clear sedimentological features such as bedded channel deposits. Unfortunately, the grain size of these deposits and the associated mineral compositions of different grain-size fractions makes the chemical composition of these deposits vary significantly. This can be avoided by choosing fine-grained levee or floodplain deposits. An analysis of ten of these deposits in the Mascall Formation shows that the compositions cluster in a distinct field that has been averaged to give the secondary parent. Secondary parent refers to the composition of the average alluvial detritus prior to final *in situ* weathering. Finally, in an effort to normalize these calculations to the least-altered alluvial or pyroclastic

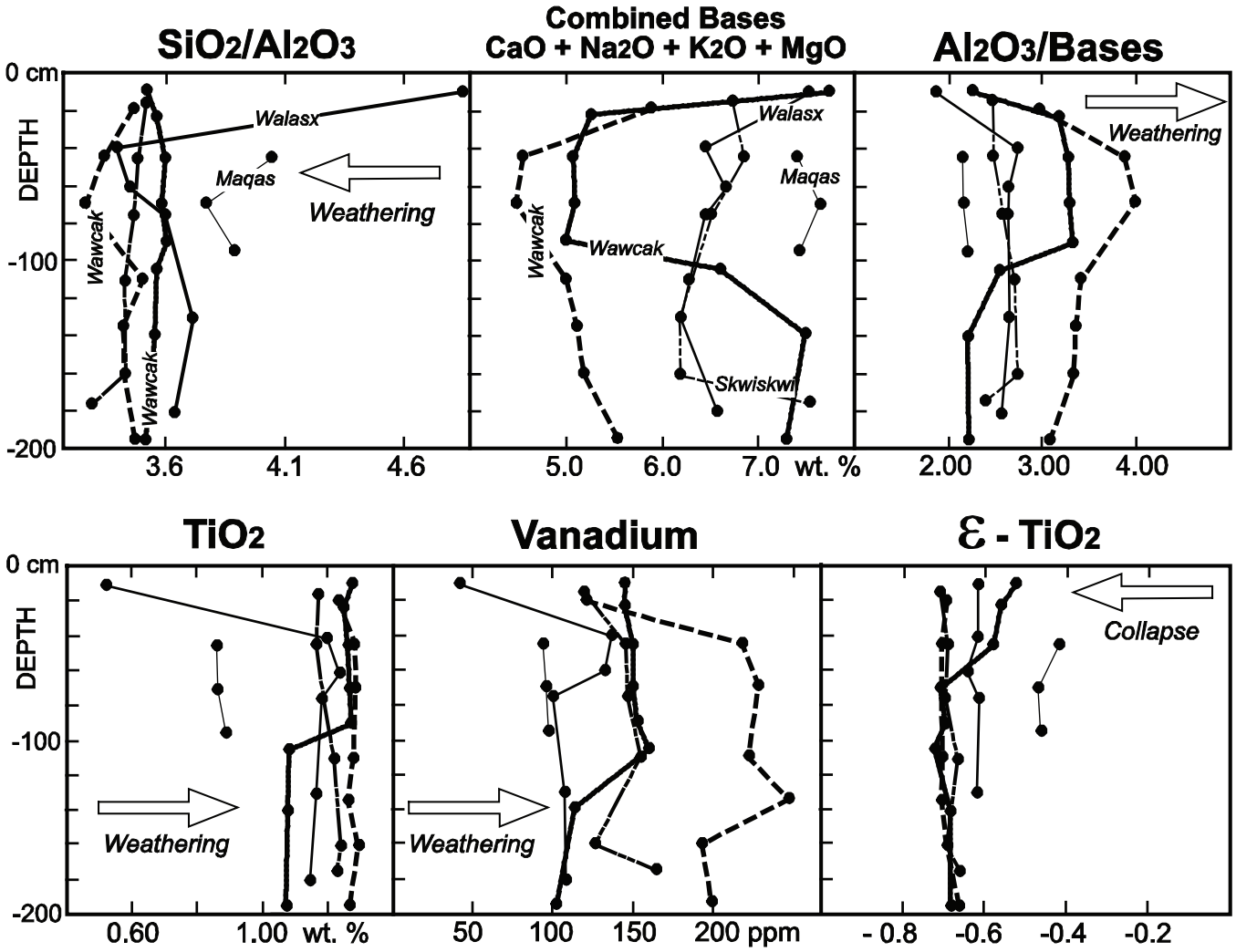

Figure 11. Geochemical depth profiles for Walasx, Skwiskwi, Maqas and two Wawcak profiles. Ratios of SiO_2/Al_2O_3 indicate clay formation and de-silication, combined bases (CaO, Na_2O, K_2O, and MgO) indicate weathering or degree of unaltered volcanic detritus, Al_2O_3/Bases indicates clay formation and leaching, TiO_2 and vanadium concentration indicates residual accumulation, and ε–TiO_2 illustrates the degree of collapse assuming a parent composition of rhyodacitic tuff.

deposit in the formation, tuffaceous beds were analyzed. The tuff bed that best represents fresh volcanic material was then chosen to be the "primary parent," similar to methods used to analyze John Day Formation strata (Bestland 2000). Because all tuff beds in the Mascall Formation show evidence of reworking, the chemical composition that best fits rhyodacitic composition was chosen for primary parent. This primary parent has base cation, silica, iron, phosphorus, and titania concentrations similar to the large pyroclastic units present in the John Day Basin (Robinson et al. 1990).

The mass balance analysis of the Mascall Formation data set using the three different parent material compositions outlined above demonstrates the large amount of weathering that occurs prior to final deposition (Fig. 13A). In situ weathering shows only minor amounts of silica loss (approximately 10% or less) and in some cases shows a slight accumulation of silica and also an accumulation accompanied by a dilation. This scatter is a result of the close compositional similarities of the *in situ* parent to the weathered daughter. Small differences between them can cause the observed scatter. The least weathered horizons, namely the most tuffaceous horizons or Maqas pedotype, shows significant dilation from its *in situ* parent. This could be a result of actual dilation caused by addition of tuffaceous component during soil formation, or it could be due to compositional heterogeneity of the horizons in this profile.

When the "secondary parent" is used in the mass balance calculation, a realistic degree of weathering is calculated for the paleosol B-horizons of approximately 40% silica loss and 45% overall weathering strain (Fig. 13A). Given the high clay content of the horizons and the pervasive pedogenic clay structures, a moderate degree of geochemical weathering would be expected. The secondary parent is a much more realistic choice in an aggrading alluvial system, such as was

Table 3. XRF data and bulk densities determined for selected paleosol profiles from throughout the Mascall Formation. All values are weight percents except for Zr which is ppm.

Sample		SiO_2	Al_2O_3	Fe_2O_3	MgO	CaO	Na_2O	K_2O	TiO_2	P_2O_5	Zr	LOI	Total	Bulk d
Lower Mascall Formation														
Ma4	Bt	59.18	17.05	9.87	1.51	2.01	0.79	0.65	1.11	0.12	190.00	7.11	99.64	2.59
Ma5	Csi	64.75	15.29	5.53	0.85	2.05	1.44	1.56	0.83	0.09	192.00	7.01	99.62	
Ma6	Bt	58.30	18.50	9.10	1.60	1.80	0.60	0.60	1.20	0.10	194.00	7.69	99.64	
Ma9a1	BC	62.09	17.54	6.13	0.77	3.23	2.12	1.29	1.01	0.07	140.00	5.20	99.61	1.67
Ma9a2	Bt	59.80	16.97	8.78	1.96	2.22	0.79	1.02	1.21	0.04	210.00	6.66	99.63	1.83
Ma11	C	60.00	14.80	5.00	1.00	5.90	1.60	2.00	0.80	2.20	160.00	5.98	99.61	1.45
Ma12	Csi	63.45	15.41	5.38	1.23	2.83	2.08	1.94	0.8	0.15	170	6.07	99.6	
Middle Mascall Formation														
Ma18-1	Bw	58.69	17.49	7.31	1.46	2.61	1.62	1.33	1.18	0.16	228	7.49	99.61	
Ma18-2	Bt	58.36	16.49	8.9	1.81	2.71	1.24	1.13	1.16	0.04	210	7.54	99.59	1.80
Ma18-3	AB	58.93	17.5	8.01	1.64	2.77	1.53	1.23	1.19	0.06	220	6.5	99.58	1.76
Ma18-4	Bw	58.68	17.42	8.22	1.75	2.69	1.43	1.18	1.25	0.06	220	6.69	99.58	1.78
Ma18-5	Bt	58.45	17.46	9.17	1.87	2.33	1.17	0.99	1.26	0.04	218	6.68	99.61	
Ma20-1	Bt	58.81	17.41	9.18	1.79	2.07	1.12	1.08	1.27	0.03	221	6.61	99.6	
Ma20-3	Bt	59.71	16.7	8.76	1.87	2.17	1.17	1.11	1.2	0.03	220	6.71	99.61	1.84
Ma26-1	Bt	56.6	17.4	7.8	1.6	3	1.5	0.9	1.2	0.1	206	9.09	99.58	
Ma26-3	Bt	57.23	17.15	8.67	1.74	3	1.07	1.07	1.22	0.03	207	8.15	99.59	
Ma28-1	Bt	57.91	17.83	7.72	1.8	2.88	1.23	1.18	1.2	0.2	187	7.29	99.58	
Ma28-5	Bt	58.24	17.95	8.05	1.66	2.62	1.44	1.14	1.24	0.06	200	6.91	99.59	1.92
Ma29-1	Bt	59.41	17.27	8.54	1.62	2.17	0.99	0.95	1.31	0.06	200	6.96	99.58	1.90
Ma30	AB	59.98	16.57	6.13	1.53	3.59	1.6	0.94	1.02	1.02	190	7.69	99.62	1.58
Ma31-3	AB	56.77	18.13	6.98	1.55	4.64	1.81	0.91	1.29	0.15	160	7.19	99.61	1.40
Ma31-4	Bt	57.21	17.26	9.07	1.9	3.08	1	0.89	1.25	0.2	189	7.51	99.61	
Ma32-2	AB	59.52	16.96	7.16	1.48	3.09	1.08	0.87	1.17	1.61	170	6.99	99.54	1.88
Ma32-3	Bt	58.95	17.21	9.49	1.71	2.17	0.82	0.78	1.31	0.12	200	6.88	99.63	1.81
Upper Mascall Formation														
Ma36	Bt	59.38	17.3	8.21	1.5	2.15	1.3	1.04	1.24	0.06	208	7.24	99.61	1.81
Ma38	Bt	60.2	17.9	7.5	1.5	2	1.1	1	1.2	0.1	190	6.92	99.62	2.05
Ma39	Bt	59.66	17.49	8.32	1.48	1.64	1.58	0.77	1.2	0.06	190	7.19	99.62	1.18
Ma40	Bt	59.66	17.62	8.76	1.76	1.31	1.67	0.93	1.25	0.05	191	6.26	99.58	1.80
Ma41	Bt	58.82	18.71	8.64	1.57	0.72	1.47	0.57	1.3	0.05	197	7.51	99.66	
Ma44	Bw	59.46	17.23	8.13	1.42	2.65	1.6	0.8	1.19	0.05	185	6.88	99.64	1.94
Ma45	Bt	58.28	17.49	8.21	1.43	3.14	1.51	0.8	1.24	0.03	192	7.03	99.63	
Ma46	Bt	57.93	17.67	9.13	1.61	2.51	1.21	0.68	1.33	0.14	199	7.24	99.65	1.91

the Mascall Formation floodplain because B-horizons are commonly superimposed on underlying B-horizons. In other words, it is rare to find an alluvial deposit with a C-horizon that has not previously been a B horizon.

Finally, in order to show the maximum degree of weathering achieved in the basin as a whole, and in order to normalize the degree of weathering so that these results can be compared to a standard and to other John Day Basin units, the least weathered or freshest volcanic material was used as a primary parent. Calculations using this parent for the most weathered paleosols show silica loss of approximately 65% and overall weathering strain of approximately 70%. These results are significantly higher than those from the secondary parent. These results can be compared to other John Day Basin units and compare well to paleosols in the upper Big Basin Member of the John Day Formation (Bestland 2000). The paleosols in the Mascall Formation are similar in overall characteristics to this member and share similar pedotypes.

Phosphorus Addition: Evidence of Andisols—Vitric fragments common to many of the Inceptisol and Alfisol-like fossil soils suggest that these fossil soils could have had andic soil properties. Andisols are found today in a wide variety of climatic settings where pyroclastic and/or volcaniclastic material is abundant (Ohmasa 1964, Wright 1964). Dis-

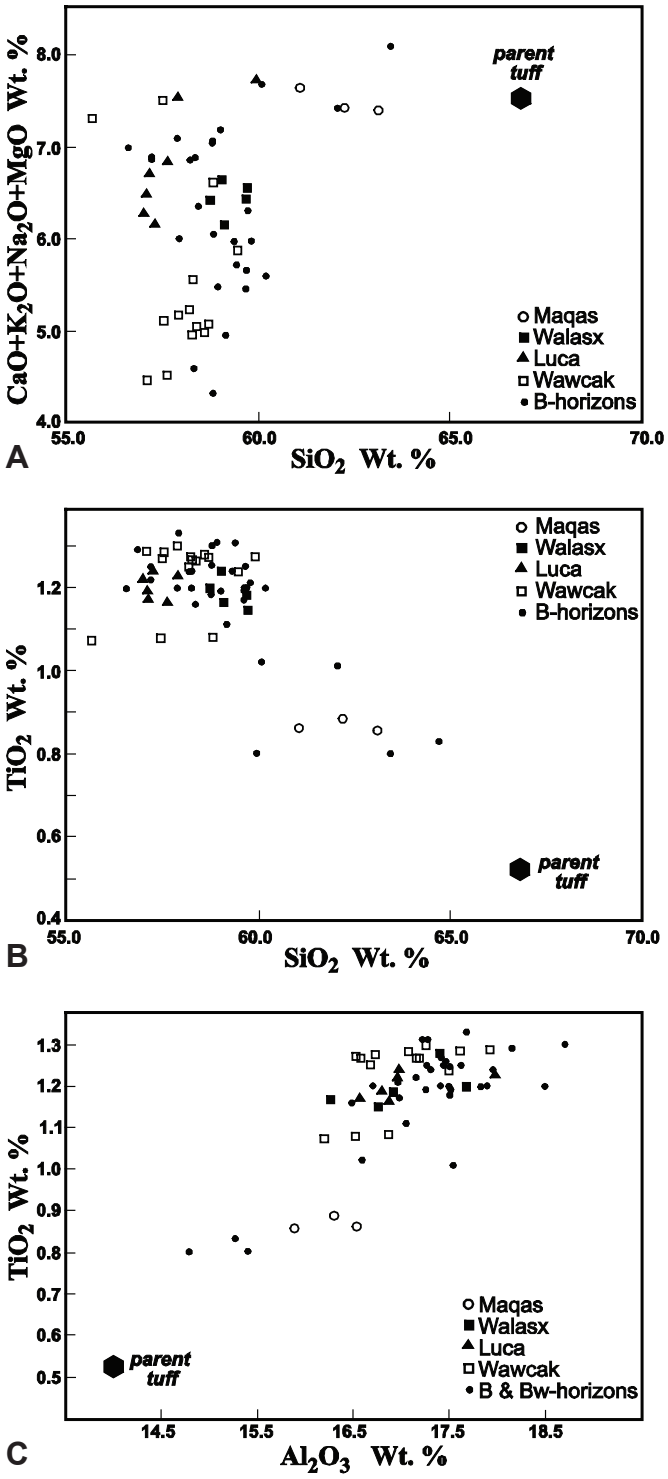

Figure 12. Scatter plots of bulk rock geochemistry of Mascall Formation paleosols and tuffaceous beds.

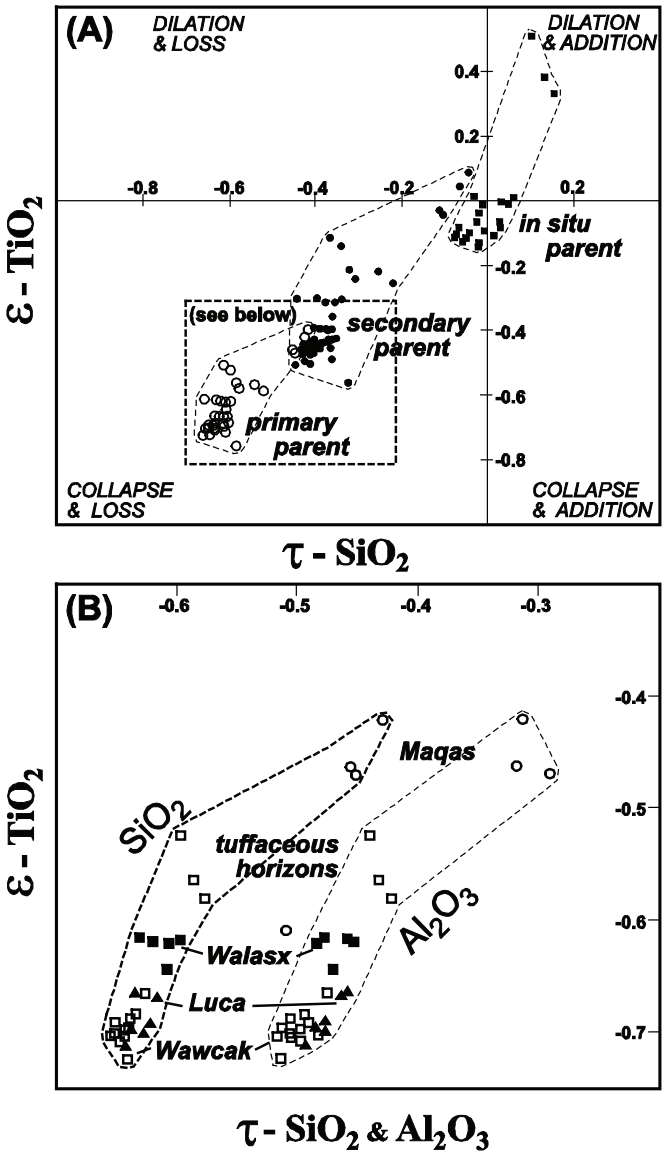

Figure 13. Pedogenic strain based on TiO_2 immobility and mass transport plots of SiO_2 and Al_2O_3 for Mascall Formation paleosols.

tinguishing characteristics of Andisols include amorphous weathering products (e.g., allophane), low bulk density, and high soil organic matter (SOM) contents (Soil Survey Staff 1998) from which the soil order received its name (in Japanese, "an" means dark or black; "do" means soil). SOM contents of 6–7% are common in tropical Andisols (Tan and van Schuylenborgh 1961), although some well-drained soils in Japan contain 15–20% (Wada and Aomine 1973). Other characteristics of Andisols are high phosphorus retention (Jones et al. 1979, Pardo et al. 1992) and low concentrations of elemental Al and Fe in soil solutions, as well as complexing of these elements with organic matter (Shoji and Fujiwara 1984, Parfitt and Kimble 1989, Aran et al. 2001). Clear Andisol-like soil features such as high SOM content, abundant amorphous weathering products, and low bulk densities are rarely preserved in the geologic record. However, phosphorus addition, iron loss, and vitric textures in John Day Formation paleosols have been used as evidence of Andisol-like soil characteristics (Bestland 2002). A few fossil soil horizons in the Mascall Formation show robust phosphorus addition (Fig. 14B); however, only a few horizons show iron loss (Fig. 14A). Iron loss was an important feature of Turtle Cove Member

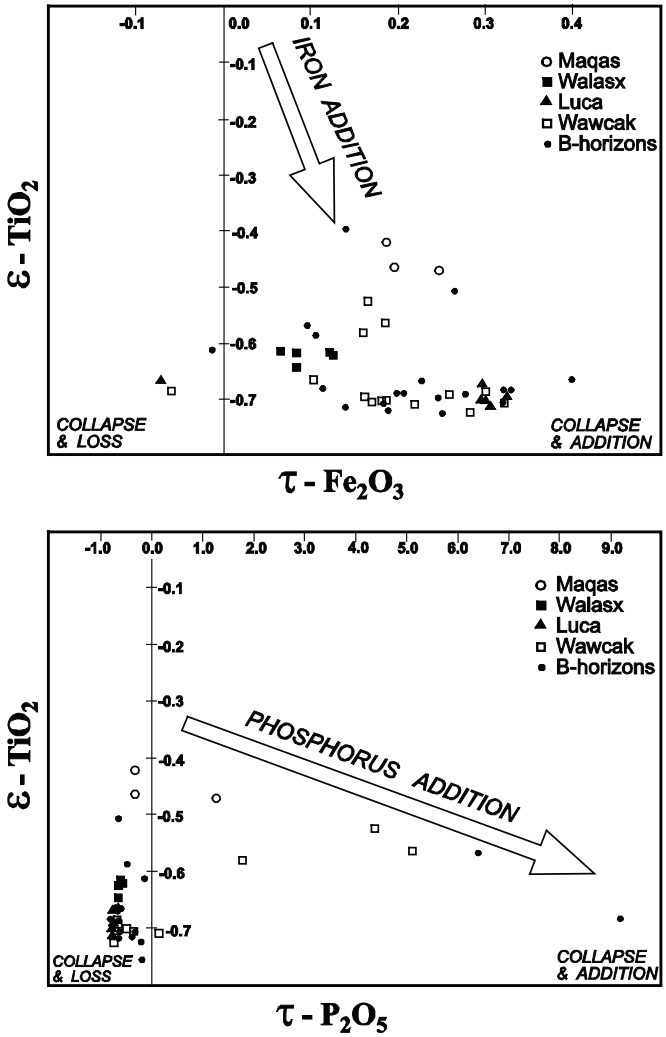

Figure 14. Pedogenic strain based on TiO_2 immobility and mass transport plots of Fe_2O_3 and P_2O_5 for Mascall Formation paleosols.

Andisol-like paleosols identified by Bestland (2002). Most of the Mascall Formation fossil soil horizons show phosphorus loss, suggesting that robust Andisol soil forming processes were not a dominant soil forming process.

PALEOENVIRONMENTAL DISCUSSION

The Mascall Formation in its type area is devoid of primary pyroclastic depositional features; all tuff beds including the Mascall Tuff Bed are either pedogenically modified or show evidence of fluvial deposition. The Mascall Tuff Bed lacks depositional structures and has an overall massive character. An en masse emplacement by gravity flow is ruled out due to the absence of coarse clasts and the presence of *in situ* pedogenic features such as burrowed structures. A more likely depositional interpretation for this unit is that of a rapidly aggrading floodplain accumulating silt-sized tuffaceous sediment from overbank flooding and windblown dust deflated from areas of bare soil and sediment.

Given the overall sedimentology of the formation, a distal volcanic source is indicated by the homogenous quality of the least pedogenically altered alluvial material, such as the Mascall Tuff Bed, as well as the lack of primary pyroclastic deposits. The geochemistry of tuffaceous units in the Mascall Formation (see previous section) and the geochemistry of John Day Formation units (Bestland et al. 1997; Retallack et al. 2000) indicate an overall rhyodacitic composition for the volcanic material coming into the basin. Two sources of this pyroclastic material are most likely—middle Miocene calderas just east of the Cascade Arc and volcanoes of the Cascade Arc to the west. A possible third source is the McDermitt volcanic field in southeast Oregon-northern Nevada. Its rhyolitic calderas date between 16.1 and 15.0 Ma (Rytuba and McKee 1984) and are thought to be the first manifestation of silicic volcanism from the Yellowstone hot spot (Pierce and Morgan 1992). As for most of the John Day Formation (i.e., its eastern and southern facies), the Mascall Formation detritus is envisioned as coming into the basin as pyroclastic airfall. The airfall deposits were then reworked, eroded and weathered by the alluvial system that formed the Mascall Formation.

Another important sedimentologic feature of the Mascall Formation is the very minor occurrence of volcanic rock fragments. Given the stratigraphic proximity and large volume of Columbia River Basalt Group rocks, and their common occurrence in the overlying Rattlesnake Formation, the rarity of basalt fragments in the Mascall Formation attests to a low-relief landscape where the Columbia River Basalt rocks would not have been a significant source of sediment. The sandy detritus in the formation is mostly of pyroclastic origin (e.g., crystal grains, pumice fragments, and rhyodacitic rock fragments), whereas the pebble and gravel detritus is mostly of pedogenic origin (pedolithic clasts). Thus, this sedimentological evidence suggests that the Mascall basin was tectonically quiet and dominated by vertical accretion and internal reworking of floodplain soils. Some of these soils had horizons that were silica-cemented or became indurated when exposed and dehydrated. This fluvial basin was contemporaneous with the extrusion to the north of the bulk of the Columbia River Basalt. The overall depositional picture that emerges for the Mascall Formation is that of a low-relief alluvial plain on the southern flank of the Columbia River Plateau (Fig. 15).

The middle Miocene had a global warm period (climatic optimum) centered around 16.0–15.0 Ma. Temperate localities in Pacific regions such as Japan and New Zealand experienced warm, almost subtropical conditions. Given that the age of the basal Mascall Formation is about 16.4 Ma, much of the unit appears to be coeval with the middle Miocene climatic optimum. The thick sequence of well-structured Luca paleosols in the middle member were hypothesized as representing the climatic optimum because balmy conditions promote clay formation and iron oxidation (Bestland and Krull 1997). However, these paleosols are not weathered to any greater degree nor do they contain higher concentrations

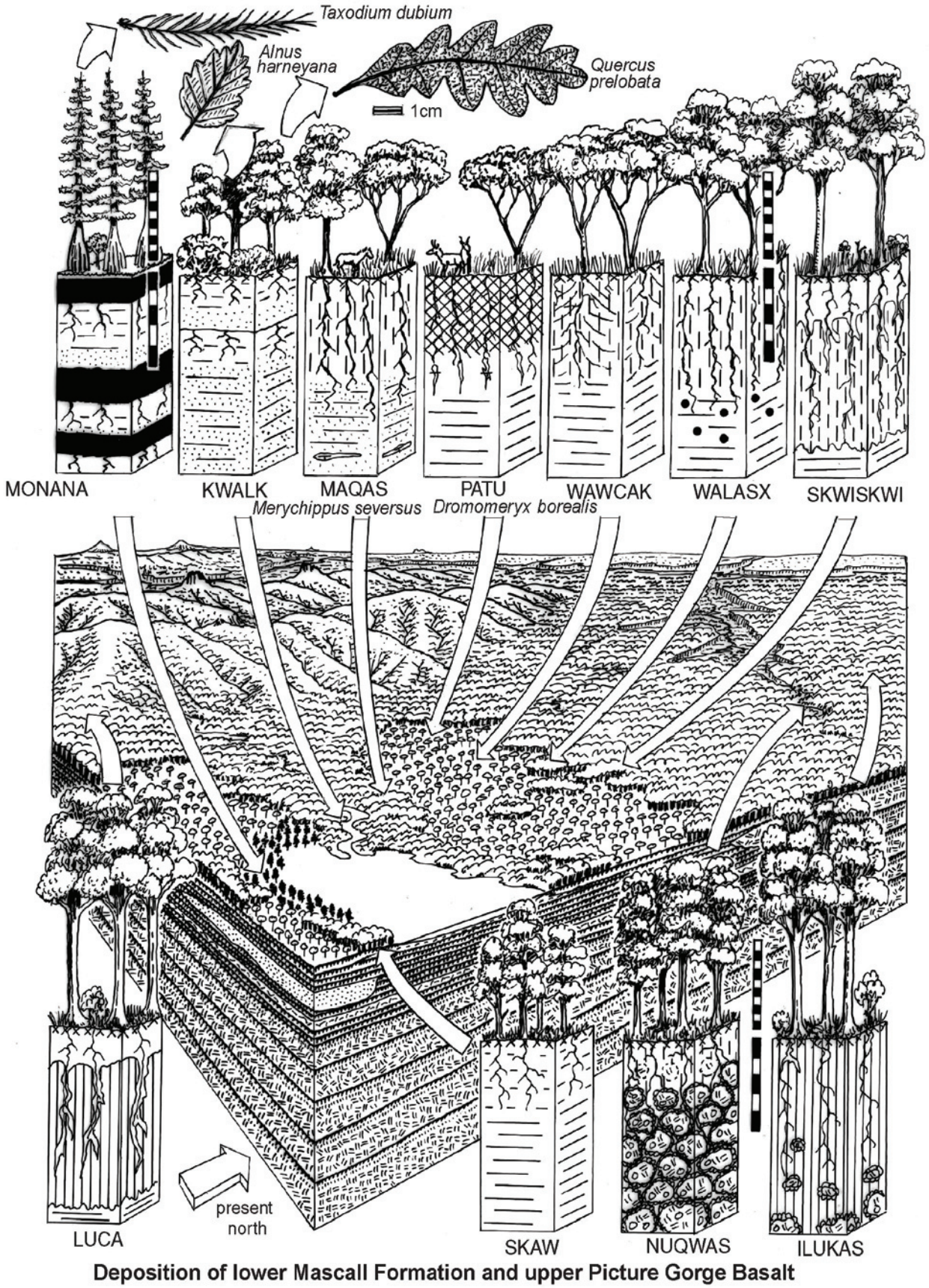

Figure 15. Paleoenvironmental reconstruction of middle Miocene Mascall time.

of iron and titanium than other well-developed paleosols in the Mascall Formation. Instead, all of the Mascall Formation in its type area may represent climatic optimum conditions, and the prominent band of red-brown paleosols would be attributed to drainage conditions conducive to the oxidation and dehydration of iron.

Distinctive stratigraphic packages of paleosols are present in all three members of the Mascall Formation. These are the maturing-upward and fining-upward paleosol sequences that average 3–5 meters thick and contain 4–6 well-developed, Alfisol- and Vertisol-like paleosols. Extrapolating from the modern soils database compiled by Birkeland et al. (1991), the Alfisols and Vertisols with Bt horizons in the Mascall Formation would have taken 10,000–50,000 years to form. Assuming an average of 20,000 years for each Bt horizon to form, these sequences would represent about 100 ka. This periodicity is similar to the 100 ka Milankovitch periodicity that appears to have forced late Pleistocene climate. During the middle Miocene, high-resolution oxygen and carbon isotope data from marine cores have a 100 ka periodicity that has been interpreted as a Milankovitch-forced global climate signal (Flower and Kennett 1994). Considering these interpretations, a possible scenario is as follows: 100 ka Milankovitch periodicity forces global climate and causes major episodes of Antarctic glaciation with a consequent global cooling feedback similar to the late Pleistocene feedbacks. Climates in the mid-latitude Pacific Northwest become cooler and drier resulting in decreased weathering rates and increased alluvial destabilization and sedimentation rates that, in turn, resulted in widespread channel-levee deposits and weakly developed Maqas type paleosols, common at the base of fining-upward sequences. Following a short glacial maximum, global climate warms, landscapes stabilize with increased vegetative cover, alluvial sedimentation rates decrease, and weathering rates increase. Alfisol and Vertisol type soils form on the stable floodplains over long periods of time (10,000s of years) in which the Skwiskwi, Wawcak, and Luca paleosols developed.

Direct integration of paleobotany with the fossil soils identified here is not possible because the vast majority of leaf fossils from the Mascall Formation in its type area occur in the lacustrine-paludal beds at the base of the formation. Leaf fossils collected from the lower and middle members of the formation are scattered and sparse, and consist of typical Mascall flora (Krull 1998). In Chaney's 1925 account of the Mascall flora, he suggests comparison with oak-madrone forests of northern coastal California. Oliver (1936) also notes that it resembles a typical Redwood border forest and compares it to forests along Big Sur River, Monterey County, California. Later, and perhaps more accurately, Chaney (1956) modified his earlier interpretation, taking into account the abundance of swamp cypress, black oak, and hickory, and compared it to the deciduous forests of the Ohio River Basin and Szechuan China, both with colder winters than coastal California. However, the humid continental environment evidenced by the paleobotanical records is inconsistent with the duric soil features common to many of the Maqas paleosols and to the silicified pedogenic conglomerate clasts common in the middle and upper members. Duric soil features are well known from humid Mediterranean climates (Soil Survey Staff 1975). Thus, a reconciliation of the paleobotany, paleopedology, and paleogeography of the Mascall Formation would be of a humid, temperate climate with both Mediterranean climatic aspects (dry, warm summer) and continental climatic aspects (cool to cold winter). The overall moisture balance during Mascall Formation time, however, did not reach the point at which there would have been significant precipitation of calcium carbonate in the soils preserved in the type area.

ACKNOWLEDGMENTS

This project was funded by three field investigation contracts to E.A. Bestland from the John Day Fossil Beds National Monument and Bureau of Land Management. The Geological Society of America and field investigation contract from the John Day Fossil Beds to E.S. Krull also funded data collection presented here. The authors would like to thank the late Lil Mascall for kindly providing access to the Mascall badlands and for cups of coffee and scotch.

LITERATURE CITED

Aran, D., M. Gury, and E. Jeanroy. 2001. Organo-metallic complexes in an Andosol: a comparative study with a Cambisol and Podzol. *Geoderma* 99:65–79.

Axelrod, D.I. 1989. Age and origin of chaparral. *Science Series of the Museum of Los Angeles County* 34:1–19.

Bailey, M.M. 1989. Revision to stratigraphic nomenclature of the Picture Gorge Basalt Subgroup, Columbia River Basalt Group. *In* S.P. Reidel and P.R. Hooper (eds.). Volcanism and Tectonism in the Columbia River Flood Basalt Province. *Geological Society of America Special Paper* 239:67–84.

Barron, J.A., and J.G. Baldauf. 1990. Development of biosiliceous sedimentation in the North Pacific during the Miocene and early Pliocene. Pp. 43–63 in R. Tsuchi (ed.). Pacific Neogene Events. University of Tokyo Press, Tokyo.

Bestland, E.A. 1994. Reconnaissance stratigraphy of the Miocene Mascall Formation in its type area of central Oregon. Unpublished report for the National Park Service. 20 pp.

Bestland, E.A. 1997. Alluvial terraces and paleosols as indicators of early Oligocene climate change (John Day Formation, Oregon). *Journal of Sedimentary Research* 67:840–855.

Bestland, E.A. 1998. Stratigraphy of the mid-Miocene Mascall Formation (lower part) in its type area. Unpublished report for John Day Fossil Beds National Monument and Bureau of Land Management. 34 pp.

Bestland, E.A. 2000. Weathering flux and CO_2 consumption determined from paleosol sequences across the Eocene-Oligocene transition. *Palaeogeography, Palaeoclimatology, Palaeoecology* 156:301–326.

Bestland, E.A. 2002. Fossil Andisols identified with mass-balance

geochemistry (Oligocene, John Day Formation, Oregon, USA). *Journal of Sedimentary Research* 72:673–686.

Bestland, E.A., and E.S. Krull. 1997. Mid-Miocene climatic optimum recorded in paleosols from the Mascall Formation (Oregon). *Geological Society of America Abstracts with Program* 29:67.

Bestland, E.A., and M.S. Forbes. 2003. Stratigraphy and geochemistry of the mid-Miocene Mascall Formation (upper part) in its type area. Unpublished report for the John Day Fossil Beds National Monument. 49 pp.

Bestland, E.A., G.J. Retallack, A.R. Rice, and A. Mindszenty. 1996. Late Eocene detrital laterites in central Oregon: mass balance geochemistry, depositional setting and landscape evolution. *Geological Society of America Bulletin* 108:285–302.

Bestland, E.A., G.J. Retallack, and C.C. Swisher, III. 1997. Step-wise climatic change recorded in Eocene-Oligocene paleosol sequences from central Oregon. *Journal of Geology* 105:153–172.

Birkeland, P.W., M.N. Machette, and K.M. Haller. 1991. Soils as a tool for applied Quaternary geology. *Utah Geological Survey, Miscellaneous Publication* 91:1–63.

Bohme, M. 2003. The Miocene climatic optimum: evidence from ectothermic vertebrates of central Europe. *Palaeogeography, Palaeoclimatology, Palaeocology* 195:389–401.

Brimhall, G.H., and W.E. Dietrich. 1987. Constitutive mass balance relations between chemical composition, volume, density, porosity, and strain in metasomatic hydrochemical systems: results on weathering and pedogenesis. *Geochimica et Cosmochimica Acta* 51:567–587.

Brimhall, G.H., O.A. Chadwick, C.J. Lewis, W. Compston, I.S. Williams, K.J. Danti, W.E. Dietrich, M.E. Power, D. Hendricks, and J. Bratt. 1991. Deformational mass transport and invasive processes in soil evolution. *Science* 255:696–702.

Caldeira, K.G., and M.R. Rampino. 1990. Deccan volcanism, greenhouse warming and the Cretaceous/Tertiary boundary. *In* V.R. Sharpton and P.E. Ward (eds.). Global Catastrophes in Earth History: An Interdisciplinary Conference on Impacts, Volcanism, and Mass Mortality. *Geological Society of America Special Paper* 247:117–123.

Chadwick, O.A., G.H. Brimhall, and D.M. Hendricks. 1990. From a black box to a gray box—a mass balance interpretation of pedogensis. *Geomorphology* 3:369–390.

Chaney, R.W. 1925. The Mascall flora; its distribution and climatic relation. *Carnegie Institute Washington Publication* 349:23–48.

Chaney, R.W. 1952. Conifer dominants in the middle Tertiary of the John Day Basin, Oregon. *The Palaeobotanist* 1:105–115.

Chaney, R.W. 1956. The ancient forests of Oregon. Condon Lectures, Oregon State System of Higher Education, University of Oregon, Eugene, OR.

Chaney, R.W., and D.I. Axelrod. 1959. Miocene floras of the Columbia Plateau. *Carnegie Institution of Washington Publications* 617:1–237.

Delancy, S., C. Genetti, and N. Rude. 1988. Some Sahaptian-Klamath-Tsimshi-anic lexical sets. Pp 195–224 *in* W. Shipley (ed.). In Honor of Mary Haas: From the Haas Festival Conference on Native American Linguistics. Mouton de Gruyter, Berlin, Germany.

Downs, T. 1956. The Mascall fauna from the Miocene of Oregon. *University of California Publications in Geological Sciences* 31:199–354.

Fiebelkorn, R.B., G.W. Walker, N.S. MacLeod, E.H. McKee, and J.G. Smith. 1983. Index to K-Ar determinations for the State of Oregon. *Isochron/West* 37:1–60.

Flower, B.P., and J.P. Kennett. 1993. Relations between Monterey Formation deposition and middle Miocene global cooling: Naples Beach section California. *Geology* 21:877–880.

Flower, B.P., and J.P. Kennett. 1994. The middle Miocene climatic transition: East Antarctic ice sheet development, deep ocean circulation and global carbon cycling. *Palaeogeography, Palaeoclimatology, Palaeoecology* 108:537–555.

Fremd, T., E.A. Bestland, and G.J. Retallack. 1997. John Day Basin Paleontology Field Trip Guide and Road Log. Northwest Interpretive Association, Seattle, Washington. 80 pp.

Hay, R.L. 1963. Stratigraphy and zeolitic diagenesis of the John Day Formation of Oregon. *University of California Publications in Geological Sciences* 42:199–261.

Hodell, D.A., R.M. Elmstrom, and J.P. Kennett. 1986. Latest Miocene $\rho^{18}O$ changes, global ice volume, sea level and the "Messinian salinity crisis." *Nature* 320:411–414.

Hooper, P.R., and D.A. Swanson. 1990. The Columbia River Basalt Group and associated volcanic rocks of the Blue Mountains Province. *In* G.W. Walker (ed.). Geology of the Blue Mountains Region of Oregon, Idaho, and Washington: Cenozoic Geology of the Blue Mountains Region. *United States Geological Survey Technical Paper* P1437:63–99.

Hornibrook, N.D.B. 1992. New Zealand Cenozoic marine paleoclimates: a review based on the distribution of some shallow water and terrestrial biota. Pp. 83–106 *in* R. Tsuchi and J.C. Ingle, Jr. (eds.). Pacific Neogene Environments, Evolution and Events. University of Tokyo Press, Tokyo.

Hsü, K.J., L. Montadert, D. Bernulli, M.B. Cita, A. Erickson, R.E. Garrison, R.B. Kidd, F. Melieres, C.X. Muller, and R. Wright. 1977. History of the Mediterranean salinity crisis. *Nature* 261:399–403.

Itoigawa, J., and T. Yamanoi. 1990. Climatic optimum in the mid-Neogene of the Japanese Islands. Pp. 3–14 in R. Tsuchi (ed.). Pacific Neogene Events. University of Tokyo Press, Tokyo.

Jones, J.P., B.B. Singh, M.A. Fosberg, and A.L. Falen. 1979. Physical, chemical and mineralogical characteristics of soils from volcanic ash, northern Idaho. *Journal of the Soil Science Society of America* 43:547–552.

Keigwin, L.D. 1980. Palaeoceanographic change in the Pacific at the Eocene-Oligocene boundary. *Nature* 287:722–725.

Kennett, J.P. 1986. Miocene to early Pliocene oxygen and carbon isotope stratigraphy in the southwest Pacific, Deep Sea Drilling Project Leg 90. *Initial Reports Deep Sea Drilling Project* 90:1383–1411.

Krull, E.S. 1998. Stratigraphy and collection of leaf-bearing units in the Miocene Mascall Formation, central Oregon. Unpublished

report for John Day Fossil Beds National Monument. 24 pp.

Kuiper, J.L. 1988. Stratigraphy and sedimentary petrology of the Mascall Formation, Eastern Oregon. M.S. thesis, Oregon State University, Corvallis, OR.

Long, P.E., and R.A. Duncan. 1982. Ar^{40}/Ar^{39} ages of Columbia River Basalt from deep boreholes in south-central Washington. Richland, Washington, Rockwell Hanford Operations Report RHO-BW-SA 233P, 11 pp.

Marincovich, L., Jr. 1990. Marine glaciation in southern Alaska during the early middle Miocene climatic optimum. Pp. 23–40 in R. Tsuchi (ed.). Pacific Neogene Events. University of Tokyo Press, Tokyo.

Merriam, J.C., C. Stock, and C.L. Moody. 1925. The Pliocene Rattlesnake Formation and fauna of eastern Oregon, with notes on the geology of the Rattlesnake and Mascall deposits. *Publications of the Carnegie Institute of Washington* 347:43–92.

Mildenhall, D.C., and D.T. Pocknall. 1984. Palaeobotanical evidence for changes in Miocene and Pliocene climates in New Zealand. Pp. 159–171 *in* J.C. Vogel (ed.). Late Cainozoic Palaeoclimates of the Southern Hemisphere: Proceedings of an International Symposium held by the South African Society for Quaternary Research, Swaziland, 29 August–2 September 1983. A.A. Balkema, Rotterdam, The Netherlands.

Mildenhall, D.C., and D.T. Pocknall. 1989. Miocene-Pleistocene spores and pollen from central Otago, South Island, New Zealand. *New Zealand Geological Survey Palaeontological Bulletin* 59:125 pp.

Miller, K.G., 1992. Middle Eocene to Oligocene stable isotope, climate and deep-water history: the terminal Eocene event? Pp. 160–177 *in* D.R. Prothero, and W.A. Berggren (eds.). Eocene-Oligocene Climatic and Biotic evolution. Princeton University Press, Princeton, New Jersey.

Miller, K.G., R.G. Fairbanks, and G.S. Mountain. 1987. Tertiary oxygen isotope synthesis, sea level history, and continental margin erosion. *Paleoceanography* 2:1–19.

Miller, K.G., J.D. Wright, and R.G. Fairbanks. 1991. Unlocking the ice house: Oligocene-Miocene oxygen isotopes, eustasy, and margin erosion. *Journal of Geophysical Research* 96:6829–6848.

Munsell Color. 1975. Munsell Color Charts; Munsell, Baltimore, Maryland, 24 p.

Ohmasa, M. 1964. Genesis and morphology of volcanic ash soils. *World Soil Resources Reports* 14:56–60.

Oliver, E.S. 1936. A Miocene flora from the Blue Mountains, Oregon. *Carnegie Institution of Washington, Contributions to Paleontology* 455:1–27.

Pardo, M.T., M.E. Guadalix, and M.T. Garcia-Gonzalez. 1992. Effect of pH and background electrolyte on P sorption by variable charge soils. *Geoderma* 54:275–284.

Parfitt, R.L., and J.M. Kimble. 1989. Conditions for formation of allophane in soils. *Journal of the Soil Science Society of America* 53:971–977.

Pierce, K.L., and L.A. Morgan. 1992. The track of the Yellowstone hot spot: volcanism, faulting, and uplift. *In* P.K. Link, M.A. Kuntz, and L.B. Platt (eds.). Regional geology of eastern Idaho and western Wyoming. *Geological Society of America Memoir* 179:1–52.

Prothero, D.R. 1994. Paradise Lost: The Eocene-Oligocene Transition. Columbia University Press, New York. 283 pp.

Prothero, D.R., Draus, E., and S.E. Foss. 2006. Magnetic stratigraphy of the lower portion of the middle Miocene Mascall Formation, central Oregon. *PaleoBios* 26(1):37–42.

Rea, D.K., M. Leinen, and T.R. Janacek. 1985. Geologic approach to the long term history of atmospheric circulation. *Science* 227:721–725.

Retallack, G.J. 1991a. A field guide to mid-Tertiary paleosols and paleoclimatic changes in the high desert of central Oregon-Part I. *Oregon Geology* 53:51–59.

Retallack, G.J. 1991b. A field guide to mid-Tertiary paleosols and paleoclimatic changes in the high desert of central Oregon-Part II. *Oregon Geology* 53:61–66.

Retallack, G.J. 1994. A pedotype approach to latest Cretaceous and earliest Tertiary paleosols in eastern Montana. *Geological Society of America Bulletin* 106:1377–1397.

Retallack, G.J. 1997. Neogene expansion of North American prairie. *Palaios* 12:380–390.

Retallack, G.J. 2004. Late Miocene climate and life on land in Oregon within a context of Neogene global change. *Palaeogeography, Palaeoclimatology, Palaeoecology* 214:97–123.

Retallack, G.J., E.A. Bestland, and T. Fremd. 2000. Eocene and Oligocene paleosols of central Oregon. *Geological Society of America Special Paper* 344:192 pp.

Rigsby, B.J. 1965. Linguistic relations in the southern Columbia plateau. Ph.D. diss. University of Oregon, Eugene, OR.

Robinson, P.T., G.F. Brem, and E.H. McKee. 1984. John Day Formation of Oregon: a distal record of early Cascade volcanism. *Geology* 12:229–232.

Robinson, P.T., G.W. Walker, and E.H. McKee. 1990. Eocene (?), Oligocene and lower Miocene rocks of the Blue Mountains region. *In* G.W. Walker (ed.). Geology of the Blue Mountains region of Oregon, Idaho, and Washington: Cenozoic Geology of the Blue Mountains Region. *U.S. Geological Survey Professional Paper* 1437:29–61.

Rytuba, J.J., and E.H. McKee. 1984. Peralkaline ash flow tuffs and calderas of the McDermitt volcanic field, southwest Oregon and north central Nevada. *Journal Geophysical Research* 89:8616–8628.

Savin, S.M., R.G. Douglas, and F.G. Stehli. 1975. Tertiary marine paleotemperatures. *Geological Society of America Bulletin* 86:1499–1510.

Sheldon, N.D. 2003. Pedogenesis and geochemical alteration of the Picture Gorge subgroup, Columbia River Basalt, Oregon. *Geological Society of America Bulletin* 115:1377–1387.

Sheldon, N.D. 2006. Using paleosols of the Picture Gorge Basalt to reconstruct the middle Miocene climatic optimum. *PaleoBios* 26(2):27–36.

Shoji, S., and Y. Fujiwara. 1984. Active Al and Fe in the humus horizons of Andosols from northwestern Japan: their forms, properties, and significance in clay weathering. *Soil Science* 137:216–226.

Soil Survey Staff. 1975. Soil taxonomy, a basic system of soil clas-

sification for making and interpreting soil surveys. U.S. Department of Agriculture Handbook 436. 754 pp.

Soil Survey Staff. 1998. Keys to Soil Taxonomy, Eighth Edition. U.S. Government Printing Office, Washington, D.C. 324 pp.

Stothers, R.B., and M.R. Rampino. 1990. Periodicity in flood basalts, mass extinctions and impacts: a statistical view and a model. *In* V.R. Sharpton and P.E. Ward (eds.). Global catastrophes in Earth history. *Special Paper of the Geological Society of America* 247:9–17.

Streck, M.J., and A. Grunder. 1995. Crystallization and welding variations in a widespread ignimbrite sheet; the Rattlesnake Tuff, eastern Oregon, USA. *Bulletin of Volcanology* 57:151–169.

Streck, M.J., J.A. Johnson, and A. Grunder. 1999. Field guide to the Rattlesnake Tuff and high lava plains near Burns. Oregon. *Oregon Geology* 61:64–76.

Tan, K.H., and J. van Schuylenborgh. 1961. On the classification and genesis of soils developed over acid volcanic materials under humid tropical conditions. II. *Netherlands Journal of Agricultural Science* 9:41–54.

Taylor, G., F. Gasse. P.H. Walker, and P.J. Morgan. 1990. The palaeoecological and palaeoclimatic significance of Miocene freshwater diatomite deposits from southern New South Wales, Australia. *Palaeogeography, Palaeoclimatology, Palaeoecology* 77:127–143.

Thayer, T.P., and R.L. Ray. 1950. Preliminary notes on later Miocene volcanism in the John Day region, Oregon. *Northwest Science* 24:89–90.

Tsuchi, R. 1990. Neogene events in Japan and the Pacific. *Palaeogeography, Palaeoclimatology, Palaeoecology* 77:355–365.

Tsuchi, R. 1992. Pacific Neogene climatic optimum and accelerated biotic evolution in time and space. Pp. 237–251 *in* R. Tsuchi and J.C. Ingle, Jr. (eds.). Pacific Neogene Environments, Evolution and Events. University of Tokyo Press, Tokyo.

van Landingham, S.L. 1964. Miocene non-marine diatoms from the Yakima region in south central Washington. *Beihefte zur Nova Hedwigia* 14:1–78.

Vincent, E., and W.H. Berger. 1982. Carbon dioxide and polar cooling in the Miocene: the Monterey hypothesis. *In* E.T. Sundquist and W.S. Broecker (eds.). The Carbon Cycle and Atmospheric CO_2: Natural Variations Archean to Present. *American Geophysical Union, Geophysical Monograph Series* 32:13–27.

Wada, K., and S. Aomine. 1973. Soil development on volcanic materials during the Quaternary. *Soil Science* 116:170–177.

Webb, S.D. 1977. A history of savanna vertebrates in the New World, Part I, North America. *Annual Reviews of Ecology and Systematics* 8:355–380.

Wolfe, J.A. 1978. A paleobotanical interpretation of Tertiary climates in the northern hemisphere. *American Scientist* 66:694–703.

Wolfe, J.A. 1981. Paleoclimatic significance of the Oligocene and Neogene floras of the northwestern United States. Pp. 79–101 *in* K.J. Niklas (ed.). Paleobotany, Paleoecology, and Evolution. Praeger Publishers, New York.

Woodruff, F., and S.M. Savin. 1991. Mid-Miocene isotope stratigraphy in the deep sea: high-resolution correlations, paleoclimatic cycles, and sediment preservation. *Paleoceanography* 6:755–806.

Woodruff, F., S.M. Savin, and R.G. Douglass. 1981. Miocene stable isotope record: a detailed deep Pacific Ocean study and its paleoclimatic implications. *Science* 212:355–380.

Wright, A.C.S. 1964. The Andosols or humic allophane soils of South America. *World Soil Resources Report* 14:9–22.

Wright, J.D., K.G. Miller, and R.G. Fairbanks. 1992. Early and middle Miocene stable isotopes: implications for deep water circulation and climate. *Paleoceanography* 7:357–389.

Zachos, J.C., J.R. Breza, and S.W. Wise. 1991. Early Oligocene ice sheet expansion on Antarctica: stable isotope and sedimentological evidence from Kerguelen Plateau, southern Indian Ocean. *Geology* 20:569–573.

Zachos, J.C., K.C. Lohmann, J.C.G. Walker, and S.W. Wise. 1993. Abrupt climate change and transient climates during the Paleogene: a marine perspective. *Journal of Geology* 101:191–213.

Zachos, J.C., M. Pagani, L. Sloan, E. Thomas, and K. Billups. 2001. Trends, rhythms, and aberrations in global climate 65 Ma to present. *Science* 292:686–693.